

**Diatom flux reflects
water-mass
conditions**

J. Onodera et al.

Diatom flux reflects water-mass conditions on the southern Northwind Abyssal Plain, Arctic Ocean

J. Onodera¹, E. Watanabe¹, N. Harada¹, and M. C. Honda²

¹Research and Development Center for Global Change, Japan Agency for Marine-Earth Science and Technology, Natsushima-cho 2–15, Yokosuka, 237-0061, Japan

²Department of Environmental Geochemical Cycle Research, Japan Agency for Marine-Earth Science and Technology, Natsushima-cho 2–15, Yokosuka, 237-0061, Japan

Received: 1 September 2014 – Accepted: 15 September 2014 – Published: 30 October 2014

Correspondence to: J. Onodera (onoderaj@jamstec.go.jp)

Published by Copernicus Publications on behalf of the European Geosciences Union.

Title Page

Abstract

Introduction

Conclusions

References

Tables

Figures



Back

Close

Full Screen / Esc

Printer-friendly Version

Interactive Discussion



Abstract

We studied time-series fluxes of diatom particles and their relationship to hydrographic variations from 4 October 2010 through 18 September 2012 using bottom-tethered sediment trap moorings deployed at Station NAP (75° N, 162° W; 1975 m water depth) in the western Arctic Ocean. We observed clear maxima of the diatom valve flux in November–December of both 2010 and 2011, and in August 2011. Diatoms in samples were categorized into 98 taxa. The diatom flux maxima were characterized by many resting spores in November–December and by the sea ice-associated diatom *Fossula arctica* in August 2011. These assemblages along with abundant clay minerals in the samples suggest a significant influence of shelf-origin materials transported by mesoscale eddies, which developed along the Chukchi Sea shelf break. In contrast, the fluxes of total mass and diatoms were reduced in summer 2012. We hypothesize that this suppression reflects the influx of oligotrophic water originating from the central Canada Basin. A physical oceanographic model demonstrated that oligotrophic surface water from the Beaufort Gyre was supplied to Station NAP from December 2011 to early half of 2012.

1 Introduction

There are numerous studies reporting the significant influence of the recent declining trend in Arctic sea-ice extent (Stroeve et al., 2012) on marine ecosystems (i.e., Grebmeier et al., 2010; Wassmann and Reigstad, 2011; Wassmann et al., 2011). The sea-ice decrease and related oceanographic changes, such as increases in water temperature, allow enhanced primary production in the Chukchi Sea (Wang et al., 2013). Diatoms are one of the major phytoplankton in the Chukchi Sea (Coupel et al., 2012), and the recent environmental changes have influenced the diatom flora and diatom productivity (e.g. Arrigo et al., 2008, 2012; Lowry et al., 2014). In the cryopelagic Canada Basin, where the major primary producer is picoplankton, the biogenic particle flux into

BGD

11, 15215–15250, 2014

Diatom flux reflects water-mass conditions

J. Onodera et al.

Title Page

Abstract

Introduction

Conclusions

References

Tables

Figures



Back

Close

Full Screen / Esc

Printer-friendly Version

Interactive Discussion



Diatom flux reflects water-mass conditions

J. Onodera et al.

Title Page

Abstract

Introduction

Conclusions

References

Tables

Figures



Back

Close

Full Screen / Esc

Printer-friendly Version

Interactive Discussion



the deep sea has been quite low (Honjo et al., 2010). The limited functioning of the biological pump essentially results from the low productivity of shell-bearing microplankton and zooplankton in oligotrophic waters (Honjo et al., 2010). The shell-bearing microplankton have a role as ballast for settling organic matter, and zooplankton produce fecal pellets. Both of these types of particles are important in biological pump processes.

The decrease in sea-ice cover results in the intensification of the Beaufort Gyre (McPhee, 2013) and deepening of the nutricline (Nishino et al., 2011a), whereas improved light penetration may support primary production in the deep chlorophyll maximum layer (Yun et al., 2012). In addition, the intensification of sea-surface circulation resulting from the sea-ice decline promotes lateral shelf–basin interactions (Nishino et al., 2011b; Watanabe and Hasumi, 2009). The upper water column in the Chukchi Borderland can be affected by three characteristic water-masses: Pacific water, East Siberian Shelf water, and Beaufort Gyre water (Nishino et al., 2011a). As one of the major contributors to the biological pump, diatoms in the offshore regions along the Chukchi Sea shelf are likely affected by these recent dramatic environmental changes.

Compared to the shelf and shelf slope areas of the Arctic Ocean where there have been many monitoring studies (i.e., Hargrave et al., 1989; Fukuchi et al., 1993; Wassmann et al., 2004; Forest et al., 2007, 2011; Gaye et al., 2007; Sampei et al., 2011), the year-round study of sinking biogenic particles in the Arctic Ocean basins is still limited, except for a few studies (Fahl and Nöthig, 2007; Honjo et al., 2010; O'Brien et al., 2013). In the Chukchi Borderland, the ice-tethered drifting sediment trap “S97-120m” was deployed in 1998 (Honjo et al., 2010), whereas there has been no year-round monitoring study of settling particles except for that by Watanabe et al. (2014). The only previous report on a time-series of diatom fluxes in the basin of the Arctic Ocean is that by Zernova et al. (2000), whose target region was at Station LOMO2 off the Laptev Sea.

In this paper, we present new findings on the settling flux of diatom valves and the relationships among diatom valve flux, sinking diatom flora, and upper water-mass

properties in the southern Northwind Abyssal Plain from October 2010 to September 2012. The Chukchi Sea is one of the obvious areas of retreating summer sea-ice (Stroeve et al., 2012). The present paper is the first report on diatom floral flux after the clear trend of declining sea-ice in the Arctic Ocean. We expect that the recent hydrographic changes in the western Arctic Ocean will be reflected in the settling diatom flux and associated assemblages. The objectives of this paper are (1) to report the variation in diatom flux and assemblage, and (2) to consider how hydrographic changes in the upper water column are reflected in the diatom assemblage and diatom flux in the western Arctic Ocean.

2 Materials and methods

Year-round deployments of a bottom-tethered mooring with two conical time-series sediment traps (model SMD26S-6000; Nichiyu Giken Kogyo Co. Ltd., Tokyo, Japan) were conducted twice at Station NAP on the southern Northwind Abyssal Plain (75° N, 162° W; 1975 m water depth) from 4 October 2010 through 27 September 2011 and from 4 October 2011 through 17 September 2012. The settling particles were collected for 10–15 days per sample. The record of the pressure sensor mounted on the sediment trap shows that the sediment traps were deployed at depths of about 180–260 m and 1300–1360 m. Before sediment-trap deployment, the 26 sampling cups of each trap were filled with seawater containing 4% neutralized formalin. In this study we analyzed all of the samples from shallower and deeper traps, except for some samples that contained a very low volume of trapped particles.

The recovered sediment-trap samples were sieved through a 1 mm mesh to remove swimmers (Matsuno et al., 2014), and then the fine size-fraction (less than 1 mm) was split into appropriate aliquots (1/1000) for diatom analysis by using a wet sample divider (WSD-10; McLane Research Laboratories, East Falmouth, Massachusetts, USA). One of the aliquots was filtered onto a membrane filter (0.45 µm pore size) with a 3 mm grid. The sample was desalted by rinsing with Milli-Q water, and then the sample filter

BGD

11, 15215–15250, 2014

Diatom flux reflects water-mass conditions

J. Onodera et al.

Title Page

Abstract

Introduction

Conclusions

References

Tables

Figures



Back

Close

Full Screen / Esc

Printer-friendly Version

Interactive Discussion



was dried overnight in an oven at 50 °C. Two sample filters were prepared for each sample, and then one of the filters was mounted on a microscope glass slide with Canada balsam

Diatoms on the glass slides were counted under a light microscope at 600× magnification. The other sample filter was used for scanning electron microscope observation after osmium coating. A minimum of 40 diatom valves (including resting-spore valves) were identified, usually to species or genus level. Diatom fluxes were estimated on the basis of valve counts, aliquot size, filtered area (535 mm²), area of sample filter observed, area of sediment trap opening (0.5 m²), and the sampling period (Onodera et al., 2005) (Appendix Table A1). As described in a previous microplankton flux study in the southeastern Beaufort Sea (Forest et al., 2007), the flux of diatom-derived particulate organic carbon (POC; hereafter, diatom POC flux) was estimated on the basis of diatom cell size and an equation for converting cell volume to carbon content per diatom cell (Menden-Deuer and Lessard, 2000). The method for bulk component analysis is described by Watanabe et al. (2014).

Data for sea-ice concentration and light intensity at the sea surface (or at the top of sea ice if present) around Station NAP during the sampling period were obtained from the National Centers for Environmental Prediction (NCEP)/Climate Forecast System Reanalysis (CFSR) (Saha et al., 2010). Sea surface temperature (SST) at Station NAP was derived from the National Oceanographic and Atmospheric Administration (NOAA) OI.v2 SST (Reynolds et al., 2002). Because the moored sediment trap array at Station NAP did not include equipment to measure current velocity, temperature, or salinity (i.e., acoustic Doppler current profiler [ADCP] or conductivity temperature depth [CTD] sensors), a physical oceanographic model known as the Center for Climate System Research Ocean Component Model (COCO) version 4.9 (Hasumi, 2006) was applied to estimate the condition of the upper water column in the western Arctic Ocean during the sampling period. The horizontal grid size of this pan-Arctic ice–ocean model was about 25 km, and there were 28 vertical levels. The model simulation was executed from 1979 to 2012 using the NCEP/CFSR atmospheric forcing data. Whereas

Diatom flux reflects water-mass conditions

J. Onodera et al.

Title Page

Abstract

Introduction

Conclusions

References

Tables

Figures



Back

Close

Full Screen / Esc

Printer-friendly Version

Interactive Discussion



most parts of experimental designs were the same as in Watanabe (2013) and Watanabe and Ogi (2013), the model version and atmospheric forcing dataset were changed from COCO 3.4 and NCEP1 (Kalnay et al., 1996), respectively. These simulated sea-ice and ocean fields were used as initial conditions for the seasonal experiments reported in Watanabe et al. (2014). These previous analyses suggest that the model captured the major variability in the western Arctic Ocean.

3 Results

3.1 Oceanographic features and mooring conditions

Station NAP is located at the southwestern edge of the Beaufort Gyre (Fig. 1), and is occasionally influenced by relatively oligotrophic waters of the Beaufort Gyre (Nishino et al., 2011a). The study area is in polar night from early November through early February (Fig. 2a). The CFSR shortwave radiation at the sea surface (or surface of sea ice) ranged from 0 to 378 W m^{-2} (Fig. 2a). Station NAP is located in a seasonal sea-ice zone, and is covered by sea-ice from late October through July (Fig. 2b). Sea surface temperature temporarily increased to about 2°C in early August in 2011 and 2012 (Fig. 2c).

The upper water column around the study area is categorized by four water masses (McLaughlin et al., 2011). Under the surface mixed layer (about the upper 25 m), Pacific summer water is observed at 25–100 m water depth (salinity approximately 31–32; Steele et al., 2004). Cold Pacific winter water (temperature minimum at 150 m, salinity around 33; Coachman and Barnes, 1961) is found under the Pacific summer water (100–250 m water depth). Higher salinity water originating from the Atlantic Ocean is observed under the Pacific winter water.

According to the logged data from pressure and temperature sensors attached to the sediment traps, the shallower sediment trap was moored at a water depth of 181–218 m (median, 184 m) for the first deployment period, and at 247–319 m (median, 256 m) for

Diatom flux reflects water-mass conditions

J. Onodera et al.

[Title Page](#)[Abstract](#)[Introduction](#)[Conclusions](#)[References](#)[Tables](#)[Figures](#)[Back](#)[Close](#)[Full Screen / Esc](#)[Printer-friendly Version](#)[Interactive Discussion](#)

the second (Fig. 2c). Therefore, the shallow trap was in Pacific winter water during the sampling period, except for in July 2012 (Fig. 2c and d). In July 2012, the depth of the shallower trap increased to 320 m in the warm Atlantic water layer, probably because of intensified water currents, which might have temporarily decreased the trapping efficiency for sinking particles (Matsuno et al., 2014). The deeper sediment trap was moored at 1318–1378 m for the entire sampling period.

3.2 Total mass flux and bulk components

As previously reported by Watanabe et al. (2014), the total mass flux showed clear annual maxima in November–December in both 2010 and 2011 (Fig. 2e and f). The major component of trapped particles was lithogenic silt-clay minerals (Fig. 2e). There was another peak in total mass flux in summer 2011, but this summer peak did not appear in 2012. The time-series of biogenic opal flux showed variations similar to those of total mass flux ($r = 0.93$ for shallow trap data, $n = 34$), and biogenic opal flux increased in November–December (Fig. 2e). Microscopic observation suggests that the biogenic opal in the studied material consisted mainly of diatoms and radiolarian shells (Ikenoue et al., 2014). The trap samples also contained low numbers of silicoflagellate skeletons, siliceous endoskeleton of dinoflagellate genus *Actiniscus*, chrysophyte cysts, ebridian flagellate, and palmals. The contribution of these siliceous flagellates to POC and biogenic opal fluxes in this study appears minor compared to the contribution from diatoms and radiolaria. This result is different from a previous study that showed a significant contribution by small flagellates to the POC flux on the Mackenzie Shelf in the southeastern Beaufort Sea (Forest et al., 2007).

3.3 Diatom valve flux and species composition

The total diatom flux captured in the shallow trap showed clear seasonality (Fig. 3a). A relatively high flux of diatom valves was observed in November–December 2010, August–September 2011, and November–December 2011 (Fig. 3a). The sinking di-

Title Page

Abstract

Introduction

Conclusions

References

Tables

Figures



Back

Close

Full Screen / Esc

Printer-friendly Version

Interactive Discussion



atom flux rapidly increased in August 2011, when the sea-ice retreated at Station NAP (Figs. 2b and 3a). The maximum of the total diatom flux at the shallow trap depth in summer 2011 reached 11.3×10^6 valves $m^{-2} d^{-1}$ in the period from 18 to 31 August. This maximum was approximately 28 % of the diatom flux maximum at Station LOMO2 (150 m trap depth) in summer 1996 (Zernova et al., 2000). In 2012, a seasonal increase in total diatom flux started after June. However, in contrast to summer 2011, there was no clear maximum of diatom flux in June–September 2012. In contrast, the flux maximum in early winter 2010 and 2011 reached 17.5×10^6 valves $m^{-2} d^{-1}$ and 10.8×10^6 valves $m^{-2} d^{-1}$, respectively. The seasonality in total diatom flux at the deep trap depth was similar to that at the shallow trap depths (Fig. 3a and b).

The diatoms found in all samples examined were categorized into 98 taxa (Table 1). The genera *Thalassionema* and *Chaetoceros* (subgenus *Hyaloch*) were the major components in shallow trap samples from late October 2010 to early July 2011 and from late November 2011 to early July 2012 (Fig. 3c, Table A1). The relative abundances of *Fragilariopsis banica* and *F. cylindrus*, which are sea ice-related diatom species (Ren et al., 2014), gradually increased from April to August 2011. The sinking diatom assemblage in summer 2011 was mainly composed of *Fossula arctica*, one of the common sea-ice diatoms in the Arctic Ocean (Cremer, 1998; von Quillfeldt, 2003). After the period of *F. arctica* dominance, the relative abundance of *Proboscia eumorpha* increased in shallow trap samples in October through early November 2011 (Fig. 3c).

The sinking diatom flora during the high flux period of November–December 2011 was essentially the same as that in 2010, although the relative abundance of *Chaetoceros* resting spores was relatively minor compared to other diatoms (Fig. 3a and b). The observed dominance of sea ice-related diatoms was low in summer 2012. Instead, relative abundance of planktic diatoms such as *Thalassiosira* spp. and *Nitzschia* spp. increased in settling diatom assemblage in summer 2012. *Melosira arctica*, which was commonly observed at Station LOMO2 (Zernova et al., 2000) and under summer sea ice in the Amundsen and Nansen basins (Boetius et al., 2013), was rarely observed in the studied samples. The diatoms encountered are mainly marine planktic and sea

Diatom flux reflects water-mass conditions

J. Onodera et al.

Title Page

Abstract

Introduction

Conclusions

References

Tables

Figures



Back

Close

Full Screen / Esc

Printer-friendly Version

Interactive Discussion



~~ice-related species. Because diatom species usually observed in fresh or low salinity water were very rare,~~ the biogenic materials collected in this study were primarily of marine origin. It has been reported that *Neodenticula seminae* is an endemic species in the subarctic North Pacific (Hasle, 1976; Yanagisawa and Akiba, 1990) and has been expanding its distribution to the North Atlantic Ocean via the Arctic Ocean since 1999 (Reid et al., 2007). At Station NAP, *N. seminae* frustules and their fragments were sporadically observed in both shallow and deep trap samples (Fig. 3c and d). Some diatom valves were observed within aggregated clay minerals, which are considered an allochthonous component originating from the Chukchi Sea shelf.

3.4 Sinking speed

Using the time-lag between the observed flux maxima at the shallow and deep trap depths, we estimated the average sinking speed of aggregated diatom particles between these depths at 37–75 m d⁻¹ in November 2010 and > 85 m d⁻¹ in August 2011. The faster sinking speed in August 2011 was primarily due to the abundant gelatinous material of zooplanktonic origin and the larger particle sizes resulting from chains of the diatoms *Fossula arctica* and *Fragilariopsis* spp.

3.5 Diatom POC flux

In order to estimate the diatom contribution to POC flux, the diatom POC flux is required instead of the flux data for diatom valve abundance. Time-series fluctuations in the diatom POC flux and in the dominant taxa in diatom POC estimation differ from those of the diatom valve flux because of the temporary increases in the flux of larger centric diatoms (Figs. 3 and 4). The estimated diatom POC flux is based on observed valve numbers. It is therefore difficult to estimate the influence of selective decomposition of diatom valves and diatom carbon on the POC flux during the sinking process. In November–December during the year of this study, the major taxa comprising diatom POC were *Coscinodiscus*, *Rhizosolenia*, and *Chaetoceros* (resting spores) (Fig. 4).

BGD

11, 15215–15250, 2014

Diatom flux reflects water-mass conditions

J. Onodera et al.

Title Page

Abstract

Introduction

Conclusions

References

Tables

Figures

◀

▶

◀

▶

Back

Close

Full Screen / Esc

Printer-friendly Version

Interactive Discussion



Diatom flux reflects water-mass conditions

J. Onodera et al.

Title Page

Abstract

Introduction

Conclusions

References

Tables

Figures



Back

Close

Full Screen / Esc

Printer-friendly Version

Interactive Discussion



A temporary increase in diatom POC flux was caused by the appearance of large *Coscinodiscus* in late March and from mid-April to early May 2011. *Fossula arctica* was the primary species in diatom POC flux during August–September 2011. The high diatom POC flux from *Rhizosolenia* and *Proboscia* in November 2011 was evidenced by the abundant occurrence of the end parts of their needle-like valves rather than the abundant occurrence of intact cells. *Proboscia* was dominant in the eastern Chukchi Sea shelf waters in September–October 2010 (J. Onodera, unpublished data). The diatom POC flux in summer 2012 was composed mainly of *Thalassiosira* spp. Although vegetative *Chaetoceros* (subgenus *Hyalochaete*) and *Thalassionema* were numerically abundant, their contribution to diatom POC was relatively minor because their cell volume is smaller than that of species of *Coscinodiscus*, *Rhizosolenia*, *Proboscia*, and *Thalassiosira*.

4 Discussion

4.1 Summer diatom flux and changes in upper water masses

The diatom flux and species composition in summer 2011 and 2012 probably reflected the dominance of different water masses – shelf water or oligotrophic Beaufort Gyre water – in the upper water column. The high dominance of *Fossula arctica* at Station NAP in summer 2011 suggests the influence of Chukchi Sea shelf waters with high productivity. According to data for the biogeographic diatom distribution in the Laptev Sea, *F. arctica* is observed mainly in the sea-ice assemblage around shelf zones rather than on the basin side (Cremer, 1998). The relatively high flux of lithogenic material in 2011 also suggests that many of the particles trapped in this study originated primarily from the Chukchi Sea shelf. During October 2010, there was a high cell density of *P. eumorpha* over the eastern Chukchi Sea shelf, whereas there was a low cell density of *Proboscia* species in water samples from the southwestern Canada Basin and the Northwind Abyssal Plain (J. Onodera, unpublished data). The relative increase in *P.*

eumorpha after the period of *F. arctica* dominance in 2011 probably suggests the influence of Chukchi shelf waters on Station NAP. The transport of coastal water toward Station NAP in summer 2011 was also inferred from the trapped gelatinous zooplankton material, such as appendicularian “houses” (S. Chiba, personal communication, 2012).

In contrast to the situation in 2011, the limited influence of shelf-origin sea-ice and shelf waters around Station NAP in 2012 are evidenced by the suppressed biogenic and lithogenic particle fluxes and the rare occurrences of *F. arctica* and other coastal biogenic particles such as appendicularian houses in January–September 2012.

To examine the background mechanisms for the suppressed biogenic fluxes in summer 2012, we investigated the relationship between horizontal advection and primary productivity using a pan-Arctic ice–ocean modeling approach. The water mass properties at Station NAP should be considered to be occasionally influenced by inter-annual variability in the Beaufort Gyre circulation. Here we analyzed the results from our inter-annual experiment using the 25 km grid COCO model. We first compared the simulated sea-surface height in the western Arctic Ocean using the summertime averages in 2011 and 2012 (Fig. 5). In general, the spatial pattern of sea surface height reflects the intensity and location of the oceanic Beaufort Gyre. The COCO model demonstrated that the sea-surface height was higher over the entire western Arctic basin, and the maximum height was in summer 2012, mostly to the western side of the basin compared to summer 2011. The difference between the two years indicates that the Beaufort Gyre expanded with shifting of its center from the Canada Basin interior to the Chukchi Borderland in 2012.

The five-year time-series of ocean current direction in the surface 100 m layer shows that a northwestward current frequently prevailed east of Station NAP (Fig. 6). This situation favors the spread of shelf-origin water with high abundance of coastal diatom taxa and lithogenic materials toward the Chukchi Borderland. The model results also show that the current direction switched southwestward in December 2011. Because the central Canada Basin is known as an oligotrophic region (Nishino et al., 2011a), the transport of nutrient-poor basin water toward Station NAP would be a possible factor for

BGD

11, 15215–15250, 2014

Diatom flux reflects water-mass conditions

J. Onodera et al.

Title Page

Abstract

Introduction

Conclusions

References

Tables

Figures



Back

Close

Full Screen / Esc

Printer-friendly Version

Interactive Discussion



explaining the suppressed primary productivity in summer 2012. These model results suggest that variations in the Beaufort Gyre significantly influenced nutrient availability and the consequent biogenic fluxes at Station NAP.

4.2 Lateral advection of coastal diatoms in early winter

Based on biogeographic characteristics, much of the *Chaetoceros* resting spores and other coastal diatoms in the studied samples can be regarded as allochthonous materials transported from shelf to basin. Compared to previous studies of particulate carbon fluxes in the Arctic Ocean (summarized in Wassmann et al., 2004), the early winter maximum of POC flux in our study is unusual under conditions of sea-ice cover and polar night. No diatom flux maximum was observed in any early winter during the previous diatom flux study at Station LOMO2 (Zernova et al., 2000). Because polar diatoms show tolerance to low light intensity (Lee et al., 2008), the autumn diatom productivity probably continued under sea-ice cover and decreasing solar radiation at Station NAP after late October (Fig. 2a and b). However, the high diatom productivity and subsequent flux of settling diatoms and other biogenic particles, comparable to the summer situation, cannot be explained on the basis of the general seasonality of primary production and sinking particle flux in the seasonal sea-ice zone of the Arctic Ocean (Wassmann et al., 2004; Wassmann and Reigstad, 2011). In this study, we also observed the annual maximum of lithogenic particle flux during the period of the high flux of sinking diatoms in November–December (Figs. 2 and 3; Watanabe et al., 2014). In the early winter of 2012 year, the origin of diatom particles comprising the diatom flux maximum around Station NAP should be treated as a complex of transported shelf-origin materials and autochthonous diatoms. The dominance of *Chaetoceros* (subgenus *Hyalochaete*) spp. and their resting spores, and abundant silt-clay minerals in the studied samples, suggests the substantial influence of Chukchi Sea shelf waters.

The increased supply of coastal diatoms and lithogenic materials in early winter can be explained by several possible mechanisms for their transport from shelf to basin.

Diatom flux reflects water-mass conditions

J. Onodera et al.

Title Page

Abstract

Introduction

Conclusions

References

Tables

Figures



Back

Close

Full Screen / Esc

Printer-friendly Version

Interactive Discussion



Diatom flux reflects water-mass conditions

J. Onodera et al.

[Title Page](#)

[Abstract](#)

[Introduction](#)

[Conclusions](#)

[References](#)

[Tables](#)

[Figures](#)



[Back](#)

[Close](#)

[Full Screen / Esc](#)

[Printer-friendly Version](#)

[Interactive Discussion](#)



Re-suspension of shelf bottom materials into the upper water column would cause the continuous dominance of lithogenic materials with coastal diatom valves in the studied particles at Station NAP. In addition, suspended neritic diatoms are incorporated into sea ice and driven offshore (Róžańska et al., 2008). However, sea-ice drift and the usual re-suspension of shelf materials cannot fully explain the early winter flux maxima of diatoms and lithogenic particles at Station NAP. The high-resolution pan-Arctic Ocean model COCO demonstrated that a drifting anti-cyclonic cold eddy generated north of Point Barrow in June 2010 passed Station NAP at the 100 to 200 m water depth during late October–early December 2010 (Watanabe et al., 2014). The simulated cold eddy passage was consistent with the observed event-like cooling and deepening of the moored trap depth that we recorded in late October–December 2010 (Fig. 2c and d). In addition, this eddy continued to pull cold water from the outer shelf during the early part of its passage from off Point Barrow toward Station NAP. Therefore, the movement of the cold eddy could account for the appearance of the high proportion of shelf bottom-water at Station NAP in late October–early December (Fig. S2.2 in Watanabe et al., 2014).

Based on the observed characteristics of diatom floral fluxes and the physical oceanographic simulation, we suggest that the unique early-winter maximum of diatom flux observed in this study is primarily caused by a drifting cold eddy that developed along the shelf break off Point Barrow (Watanabe et al., 2014). Whereas eddy-induced lateral transport of coastal materials has been reported in the Canada Basin (O'Brien et al., 2011, 2013; Nishino et al., 2011b), the eddy in this study, composed of Pacific-origin waters with lower density, did not flow down the shelf slope. Because the shallow sediment trap was moored at about 260 m during the second deployment, the direct influence of the cold eddy was not detected by the temperature and pressure sensors attached to the sediment trap. However, a similar eddy-induced transport event of shelf materials to the basin in early winter 2011 is evident in the high diatom flux, the characteristic diatom assemblage, and the high abundance of lithogenic clay particles.

4.3 Role of diatoms in the biological pump

Because biogenic opal has a ballast effect on the export of particulate organic matter to deep basins (Honjo et al., 2008; Honda and Watanabe, 2010), the biological pump is usually effective in diatom-rich oceans such as the Aleutian Basin in the Bering Sea (Takahashi et al., 2002), the subarctic North Pacific (Honda et al., 2002; Takahashi et al., 2002; Honda and Watanabe, 2010), and the Southern Ocean (Honjo et al., 2008). However, most settling autochthonous POC in the central Canada Basin is remineralized within subsurface layers (Honjo et al., 2010). Fresh POC is not supplied to deeper layers, even though there is primary production of $2\text{--}4\text{ mol C m}^{-2}\text{ y}^{-1}$ (Honjo et al., 2010). The primary producers in the cryopelagic Canada Basin are mainly green algae and other picoplankton (e.g., Coupel et al., 2012). The limited amounts of diatoms supplying biogenic ballast and fecal pellets are the causes of an ineffective biological pump in the Canada Basin (Honjo et al., 2010). The relatively abundant POC fluxes at Station NAP, in comparison to those at sediment-trap Station CD04-3067 m (trap depth: 3067 m) in the central Canada Basin (Honjo et al., 2010), are due to the higher lateral carbon transport from the Chukchi Sea shelf, autochthonous production of phyto- and zooplankton around Station NAP (Watanabe et al., 2014).

The diatoms collected in our samples sometimes retained the chain form of frustules. In particular, frustules with residual protoplasm were also observed in the summer samples. Their occurrence suggests that the carbon supplied to the deep sea in the Northwind Abyssal Plain includes not only old carbon transported from the shelf or sea-floor ridge but also fresh carbon produced around the study area. When the influence of shelf-origin water is obvious at Station NAP, as in 2011, the biological pump at Station NAP will be relatively active owing to abundant supplies of biogenic and lithogenic particles. In contrast, when oligotrophic water from the central Canada Basin was supplied to Station NAP, as observed in early 2012, the sinking particle flux at Station NAP was limited. In this situation, ~~the biological pump might be suppressed~~ to a level comparable to that in the central Canada Basin. Therefore, on the Chukchi shelf

BGD

11, 15215–15250, 2014

Diatom flux reflects water-mass conditions

J. Onodera et al.

Title Page

Abstract

Introduction

Conclusions

References

Tables

Figures



Back


Close

Full Screen / Esc

Printer-friendly Version

Interactive Discussion



side of the outer Beaufort Gyre, primary productivity and the biological pump are influenced by the spatial distribution of upper water masses (Nishino et al., 2011a). When oligotrophic sea-surface waters ^{supp}  the summer particle flux, as evident in summer 2012, the eddy effect on lateral advection of shelf materials to the basin (Nishino et al., 2011b; O'Brien et al., 2011, 2013; Watanabe et al., 2014) becomes important to the seasonality of organic matter flux and the composition of the sinking microplankton flora in the study area (Watanabe et al., 2014).

Author contributions. N. Harada planned the research project. J. Onodera carried out the diatom analysis and offshore work of sediment-trap mooring experiments. E. Watanabe implemented the physical oceanographic model. M. C. Honda analyzed the biogenic opal in sediment trap samples. J. Onodera and E. Watanabe prepared the manuscript with contributions from all co-authors.

Acknowledgements. We gratefully thank the captains, crews, chief scientist, and marine technicians of R/V *Mirai* and CCGS *Sir Wilfrid Laurier* for mooring operations, and Yuichiro Tanaka for supplying sediment trap equipment. This work was funded a Grant-in-Aid for Scientific Research (S) of the Japan Society for the Promotion of Science (JSPS) JFY2010-2014, No. 22221003, "Catastrophic reduction of sea ice in the Arctic Ocean: its impact on the marine ecosystems in the polar region" to N. Harada, and by a JSPS Research Fellowship for Young Scientists to J. Onodera (No. 22-5808). Modeling experiments were executed by E. Watanabe using the Japan Agency for Marine-Earth Science and Technology (JAMSTEC) Earth Simulator version 2.

References

- Arrigo, K. R., van Dijken, G., and Pabi, S.: Impact of a shrinking Arctic ice cover on marine primary production, *Geophys. Res. Lett.*, 35, L19603, doi:10.1029/2008GL035028, 2008.
- Arrigo, K. R., Perovich, D. K., Pickart, R. S., Brown, Z. W., van Dijken, G. L., Lowry, K. E., Mills, M. M., Palmer, M. A., Balch, W. M., Bahr, F., Bates, N. R., Benitez-Nelson, C., Bowler, B., Brownlee, E., Ehn, J. K., Frey, K. E., Garley, R., Ianey, S. R., Lubelczyk, L., Mathis, J., Matsuoka, A., Mitchell, B. G., Moore, W. K., Ortega-Retuerta, E., Ppal, S.,

BGD

11, 15215–15250, 2014

Diatom flux reflects water-mass conditions

J. Onodera et al.

Title Page

Abstract

Introduction

Conclusions

References

Tables

Figures



Back

Close

Full Screen / Esc

Printer-friendly Version

Interactive Discussion



Diatom flux reflects water-mass conditions

J. Onodera et al.

[Title Page](#)

[Abstract](#)

[Introduction](#)

[Conclusions](#)

[References](#)

[Tables](#)

[Figures](#)



[Back](#)

[Close](#)

[Full Screen / Esc](#)

[Printer-friendly Version](#)

[Interactive Discussion](#)



Polashenski, C. M., Reynolds, R. A., Schieber, B., Sosik, H. M., Stephens, M., and Swift, J. H.: Massive phytoplankton blooms under Arctic sea ice, *Science*, 336, 1408, doi:10.1126/science.1215065, 2012.

Boetius, A., Albrecht, S., Bakker, K., Bienhold, C., Felden, J., Fernández-Méndez, M., Hendricks, S., Katlein, C., Lalande, C., Krumpen, T., Niclaus, M., Peeken, I., Rabe, B., Rogacheva, A., Rybakova, E., Somavilla, R., Wenzhöfer, F., and RV *Polarstern* ARK27-3-Shipboard Science Party: Export of algal biomass from the melting Arctic sea ice, *Science*, 339, 1430–1432, doi:10.1126/science.1231346, 2013.

Coachman, L. K. and Barnes, C. A.: The contribution of Bering Sea water to the Arctic Ocean, *Arctic*, 14, 147–161, 1961.

Coupel, P., Jin, H. Y., Joo, M., Horner, R., Bouvet, H. A., Sicre, M.-A., Gascard, J.-C., Chen, J. F., Garçon, V., and Ruiz-Pino, D.: Phytoplankton distribution in unusually low sea ice cover over the Pacific Arctic, *Biogeosciences*, 9, 4835–4850, doi:10.5194/bg-9-4835-2012, 2012.

Cremer, H.: The diatom flora of Laptev Sea (Arctic Ocean), *Biblioth. Diatomol.*, 40, 1–169, 1998.

Danielson, S., Curchitser, E., Hedstrom, K., Weingartner, T., and Stabeno, P.: On ocean and sea ice modes of variability in the Bering Sea, *J. Geophys. Res.*, 116, C12036, doi:10.1029/2011JC007389, 2011.

Fahl, K. and Nöthig, E.-M.: Lithogenic and biogenic particle fluxes on the Lomonosov Ridge (central Arctic Ocean) and their relevance for sediment accumulation: vertical vs. lateral transport, *Deep-Sea Res. Pt. I*, 54, 1256–1272, 2007.

Forest, A., Sampei, M., Hattori, H., Makabe, R., Sasaki, H., Fukuchi, M., Wassmann, P., and Fortier, L.: Particulate organic carbon fluxes on the slope of the Mackenzie Shelf (Beaufort Sea): physical and biological forcing of shelf-basin exchangesm *J. Marine Syst.*, 68, 39–54, 2007.

Forest, A., Galindo, V., Darnis, G., Pineault, S., Lalande, C., Tremblay, J.-E., and Fortier, L.: Carbon biomass, elemental ratios (C:N) and stable isotopic composition ($\delta^{13}\text{C}$, $\delta^{15}\text{N}$) of dominant calanoid copepods during the winter-to-summer transition in the Amundsen gulf (Arctic Ocean), *J. Plankton Res.*, 33, 161–178, 2011.

Fukuchi, M., Sasaki, H., Hattori, H., Matuda, O., Tanimura, A., Handa, N., and McRoy, C. P.: Temporal variability of particulate flux in the northern Bering Sea, *Cont. Shelf Res.*, 13, 693–704, 1993.

Diatom flux reflects water-mass conditions

J. Onodera et al.

Title Page

Abstract

Introduction

Conclusions

References

Tables

Figures



Back

Close

Full Screen / Esc

Printer-friendly Version

Interactive Discussion



Gaye, B., Fahl, K., Kodina, L. A., Lahajnar, N., Nagel, B., Unger, D., and Gebhardt, A. C.: Particulate matter fluxes in the southern and central Kara Sea compared to sediments: bulk fluxes, amino acids, stable carbon and nitrogen isotopes, sterols and fatty acids, *Cont. Shelf Res.*, 27, 2570–2594, 2007.

5 Grebmeier, J. M., Moore, S. E., Overland, J. E., Frey, K. E., and Gradinger, R.: Biological response to recent Pacific Arctic sea ice retreats, *Eos*, 91, 161–162, 2010.

Hargrave, B. T., von Bodungen, B., Conover, R. J., Fraser, A. J., Phyllips, G., and Vass, W. P.: Seasonal changes in sedimentation of particulate matter and lipid content of zooplankton collected by sediment trap in the Arctic Ocean off Axel Heiberg Island, *Polar Biol.*, 9, 467–475, 1989.

10 Hasle, G. R.: The biogeography of some marine planktonic diatoms, *Deep-Sea Res.*, 23, 319–338, 1976.

Hasumi, H.: CCSR Ocean Component Model (COCO) version 4, Center for Clim. Sys. Res. Rep., Univ. of Tokyo, 25, 1–103, 2006.

15 Honda, M. C. and Watanabe, S.: Importance of biogenic opal as ballast of particulate organic carbon (POC) transport and existence of mineral ballast-associated and residual POC in the Western Pacific Subarctic Gyre, *Geophys. Res. Lett.*, 37, L02605, doi:10.1029/2009GL041521, 2010.

20 Honda, M. C., Imai, K., Nojiri, Y., Hoshi, F., Sugawara, T., and Kusakabe, M.: The biological pump in the northwestern North Pacific based on fluxes and major components of particulate matter obtained by sediment-trap experiments (1997–2000), *Deep-Sea Res. Pt. II*, 49, 5595–5625, 2002.

Honjo, S., Manganini, S. J., Krishfield, R. A., and Francois, R.: Particulate organic carbon fluxes to the ocean interior and factors controlling the biological pump: a synthesis of global sediment trap programs since 1983, *Prog. Oceanogr.*, 76, 217–285, 2008.

25 Honjo, S., Krishfield, R. A., Eglinton, T. I., Manganini, S. J., Kemp, J. N., Doherty, K., Hwang, J., McKee, T. K., and Takizawa, T.: Biological pump processes in the cryopelagic and hemipelagic Arctic Ocean: Canada Basin and Chukchi Rise, *Prog. Oceanogr.*, 85, 137–170, 2010.

30 Ikenoue, T., Bjørklund, K. R., Kruglikova, S. B., Onodera, J., Kimoto, K., and Harada, N.: Seasonal flux changes of microzooplankton (*Radiolaria*) under the seasonally sea-ice covered conditions in the western Arctic Ocean, *Biogeosci. Discuss.*, submitted, 2014.

Diatom flux reflects water-mass conditions

J. Onodera et al.

[Title Page](#)

[Abstract](#)

[Introduction](#)

[Conclusions](#)

[References](#)

[Tables](#)

[Figures](#)



[Back](#)

[Close](#)

[Full Screen / Esc](#)

[Printer-friendly Version](#)

[Interactive Discussion](#)



- Lee, S. H., Whitledge, T. E., and Kang, S. H.: Carbon uptake rates of sea ice algae and phytoplankton under different light intensities in a landfast sea ice zone, Barrow, Alaska, Arctic, 61, 281–291, 2008.
- Lowry, K. E., van Dijken, G. L., and Arrigo, K. R.: Evidence of under-ice phytoplankton blooms in the Chukchi Sea from 1998 to 2012, *Deep-Sea Res. Pt. II*, 105, 105–117, 2014.
- Matsuno, K., Yamaguchi, A., Fujiwara, A., Onodera, J., Watanabe, E., Imai, I., Chiba, S., Harada, N., and Kikuchi, T.: Seasonal changes in mesozooplankton swimmers collected by sediment trap moored at a single station on the Northwind Abyssal Plain in the western Arctic Ocean, *J. Plankton Res.*, 36, 490–502, 2014.
- McLaughlin, F., Carmack, E., Proshutinsky, A., Krishfield, R. A., Guay, C., Yamamoto-Kawai, M., Jackson, J. M., and Williams, B.: The rapid response of the Canada Basin to climate forcing: from bellwether to alarm bells, *Oceanography*, 24, 146–159, 2011.
- McPhee, M. G.: Intensification of geostrophic currents in the Canada Basin, Arctic Ocean, *J. Climate*, 26, 3130–3138, 2013.
- Menden-Deuer, S. and Lessard, E. J.: Carbon to volume relationships for dinoflagellates, diatoms, and other protist plankton, *Limnol. Oceanogr.*, 45, 569–579, 2000.
- Nishino, S., Kikuchi, T., Yamamoto-Kawai, M., Kawaguchi, Y., Hirawake, T., and Itoh, M.: Enhancement/reduction of biological pump depends on ocean circulation in the sea-ice reduction regions of the Arctic Ocean, *J. Oceanogr.*, 67, 305–314, 2011a.
- Nishino, S., Itoh, M., Kawaguchi, Y., Kikuchi, T., and Aoyama, M.: Impact of an unusually large warm-core eddy on distributions of nutrients and phytoplankton in the southwestern Canada Basin during late summer/early fall 2010, *Geophys. Res. Lett.*, 38, L16602, doi:10.1029/2011GL047885, 2011b.
- O'Brien, M. C., Melling, H., Pedersen, T. F., and Macdonald, R. W.: The role of eddies and energetic ocean phenomena in the transport of sediment from shelf to basin in the Arctic, *J. Geophys. Res.*, 116, C08001, doi:10.1029/2010JC006890, 2011.
- O'Brien, M. C., Melling, H., Pedersen, T. F., and Macdonald, R. W.: The role of eddies on particle flux in the Canada Basin of the Arctic Ocean, *Deep-Sea Res. Pt. I*, 71, 1–20, 2013.
- Onodera, J., Takahashi, K., and Honda, M. C.: Pelagic and coastal diatom fluxes and the environmental changes in the northwestern North Pacific during December 1997–May 2000, *Deep-Sea Res. II*, 52, 2218–2239, 2005.
- Passow, U. and Carlson, C. A.: The biological pump in a high CO₂ world, *Mar. Ecol.-Prog. Ser.*, 470, 249–271, 2012.

Diatom flux reflects water-mass conditions

J. Onodera et al.

Title Page

Abstract

Introduction

Conclusions

References

Tables

Figures



Back

Close

Full Screen / Esc

Printer-friendly Version

Interactive Discussion



- Reid, P. C., Johns, D. G., Edwards, M., Starr, M., Poulin, M., and Snoeijs, P.: A biological consequence of reducing Arctic ice cover: arrival of the Pacific diatom *Neodenticula seminata* in the North Atlantic for the first time in 800 000 years, *Glob. Change Biol.*, 13, 1910–1921, 2007.
- 5 Ren, J., Gersonde, R., Esper, O., and Sancetta, C.: Diatom distributions in northern North Pacific surface sediments and their relationship to modern environmental variables, *Palaeogeogr. Palaeoclimatol.*, 402, 81–103, 2014.
- Reynolds, R. W., Rayner, N. A., Smith, T. M., Stokes, D. C., and Wang, W.: An improved in situ and satellite SST analysis for climate, *J. Climate*, 15, 1609–1625, 2002.
- 10 Rózańska, M., Poulin, M., and Gosselin, M.: Protist entrapment in newly formed sea ice in the Coastal Arctic Ocean, *J. Marine Syst.*, 74, 887–901, 2008.
- Saha, S., Moorthi, S., Pan, H.-L., Wu, X., Wang, J., Nadiga, S., Tripp, P., Kistler, R., Woollen, J., Behringer, D., Liu, H., Stokes, D., Grumbine, R., Gayno, G., Wang, J., Hou, Y.-T., Chuang, H., Juang, H.-M. H., Sela, J., Iredell, M., Treadon, R., Kleist, D., Delst, P. V., Keyser, D., Derber, J., Ek, M., Meng, J., Wei, H., Yang, R., Lord, S., van den Dool, H., Kumar, A., Wang, W., Long, C., Chelliah, M., Xue, Y., Huang, B., Schemm, J.-K., Ebisuzaki, W., Lin, R., Xie, P., Chen, M., Zhou, S., Higgins, W., Zou, C.-Z., Liu, Q., Chen, Y., Han, Y., Cucurull, L., Reynolds, R. W., Rutledge, G., and Goldberg, M.: The NCEP Climate Forecast System Reanalysis, *B. Am. Meteorol. Soc.*, 91, 1015–1057, 2010.
- 20 Sampei, M., Sasaki, H., Makabe, R., Forest, A., Hattori, H., Tremblay, J.-E., Gratton, Y., Fukuchi, M., and Fortier, L.: Production and retention of biogenic matter in the southeast Beaufort Sea during 2003–2004: insights from annual vertical particle fluxes of organic carbon and biogenic silica, *Polar Biol.*, 34, 501–511, 2011.
- Steele, M., Morison, J., Ermold, W., Rigor, I., Ortmeyer, M., and Shimada, K.: Circulation of summer Pacific halocline water in the Arctic Ocean, *J. Geophys. Res.*, 109, C02027, doi:10.1029/2003JC002009, 2004.
- 25 Stroeve, J. C., Serreze, M. C., Holland, M. M., Kay, J. E., Malanik, J., and Barrett, A. P.: The Arctic's rapidly shrinking sea ice cover: a research synthesis, *Climatic Change*, 110, 1005–1027, doi:10.1007/s10584-011-0101-1, 2012.
- 30 Takahashi, K., Fujitani, N., and Yanada, M.: Long term monitoring of particle fluxes in the Bering Sea and the central subarctic Pacific Ocean, 1990–2000, *Prog. Oceanogr.*, 55, 95–112, 2002.

Diatom flux reflects water-mass conditions

J. Onodera et al.

[Title Page](#)

[Abstract](#)

[Introduction](#)

[Conclusions](#)

[References](#)

[Tables](#)

[Figures](#)



[Back](#)

[Close](#)

[Full Screen / Esc](#)

[Printer-friendly Version](#)

[Interactive Discussion](#)



- von Quillfeldt, C. H., Ambrose Jr., W. G., and Clough, L. M.: High number of diatom species in first-year ice from the Chukchi Sea, *Polar Biol.*, 26, 806–818, 2003.
- Wang, J., Hu, H., Goes, J., Miksis-Olds, J., Mouw, C., D'Sa, E., Gomes, H., Wang, D. R., Mizobata, K., Saitoh, S., and Luo, L.: A modeling study of seasonal variations of sea ice and plankton in the Bering and Chukchi Seas during 2007–2008, *J. Geophys. Res.-Oceans*, 118, 1–14, doi:10.1029/2012JC008322, 2013.
- Wassmann, P. and Reigstad, M.: Future Arctic Ocean seasonal ice zones and implications for pelagic–benthic coupling, *Oceanography*, 24, 220–231, 2011.
- Wassmann, P., Bauerfeind, E., Fortier, M., Fukuchi, M., Hargrave, B., Moran, B., Noji, T., Nöthig, E.-M., Olli, K., Peinert, R., Sasaki, H., and Shevchenko, V.: Particulate organic carbon flux to the Arctic Ocean sea floor, in: *The Organic Carbon Cycle in the Arctic Ocean*, edited by: Stein, R. and Macdonald, R. W., Springer, Berlin, 101–138, 2004.
- Wassmann, P., Duarte, C. M., Agust, S., and Sejr, M. K.: Footprints of climate change in the Arctic marine ecosystem, *Glob. Change Biol.*, 17, 1235–1249, doi:10.1111/j.1365-2486.2010.02311.x, 2011.
- Watanabe, E.: Linkages among halocline variability, shelf-basin interaction, and wind regimes in the Beaufort Sea demonstrated in pan-Arctic Ocean modeling framework, *Ocean Model.*, 71, 43–53, doi:10.1016/j.ocemod.2012.12.010, 2013.
- Watanabe, E. and Hasumi, H.: Pacific water transport in the western Arctic Ocean simulated by an eddy-resolving coupled sea ice–ocean model, *J. Phys. Oceanogr.*, 39, 2194–2211, 2009.
- Watanabe, E. and Ogi, M.: How does Arctic summer wind modulate sea ice–ocean heat balance in the Canada Basin?, *Geophys. Res. Lett.*, 40, 1569–1574, doi:10.1002/grl.50363, 2013.
- Watanabe, E., Onodera, J., Harada, N., Honda, M. C., Kimoto, K., Kikuchi, T., Nishino, S., Mtsuno, K., Yamaguchi, A., Ishida, A., and Kishi, M. J.: An enhanced role of eddies in the Arctic marine biological pump, *Nat. Commun.*, 5, 3950, doi:10.1038/ncomms4950, 2014.
- Yanagisawa, Y. and Akiba, F.: Taxonomy and phylogeny of the three marine diatom genera, *Crucidentricula*, *Denticulopsis* and *Neodenticula*, *Bull. Geol. Surv. Japan*, 41, 197–301, 1990.
- Yun, M. S., Chung, K. H., Zimmermann, S., Zhao, J., Joo, H. M., and Lee, S. H.: Phytoplankton productivity and its response to higher light levels in the Canada Basin, *Polar Biol.*, 35, 257–268, doi:10.1007/s00300-011-1070-6, 2012.

Zernova, V. V., Nöthig, E.-M., and Shevchenko, V. P.: Vertical microalga flux in the Northern Laptev Sea (from the data collected by the yearlong sediment trap), *Oceanology*, 40, 801–808, 2000.

Discussion Paper | Discussion Paper | Discussion Paper | Discussion Paper | Discussion Paper

BGD

11, 15215–15250, 2014

Diatom flux reflects water-mass conditions

J. Onodera et al.

- Title Page
- Abstract Introduction
- Conclusions References
- Tables Figures
- ◀ ▶
- ◀ ▶
- Back Close
- Full Screen / Esc
- Printer-friendly Version
- Interactive Discussion



Table 1. Diatom taxa found in sediment trap samples from Station NAP collected from 4 October 2010 to 18 September 2012. The symbols “*” and “?” indicate sea ice-related taxa, and uncertain identification in this study, respectively.

Taxa	
<i>Achnanthes brevipes</i> Agardh (1824)	<i>Neodenticula seminiae</i> (Simonsen and Kanaya) Akiba and Yanagisawa (1986)
<i>Achnanthes lanceolata</i> (Brebisson) Grunow (1880) ?	<i>Nitzschia arctica</i> Cleve (1896) *
<i>Actinocyclus curvatulus</i> Janisch (1874)	<i>Nitzschia frigida</i> Grunow (1880) *
<i>Actinocyclus</i> spp.	<i>Nitzschia neofrigida</i> Medlin (1990) *
<i>Actinoptychus senarius</i> (Ehrenberg) Ehrenberg (1843)	<i>Nitzschia polaris</i> (Grunow) Grunow (1884) *
<i>Asteromphalus brookei</i> Bailey (1856)	<i>Nitzschia promare</i> Medlin (1990) *
<i>Asteromphalus hyalinus</i> Karsten (1905)	<i>Nitzschia seriata</i> Cleve (1883)
<i>Aulacoseira</i> spp.	<i>Nitzschia</i> spp.
<i>Bacillaria</i> spp.	<i>Odontella aurita</i> (Lyngbye) Agardh (1832)
<i>Bacterosira fragilis</i> (Gran) Gran (1900)	<i>Paralia</i> spp.
<i>Centric</i> spp.	<i>Pauliella taeniata</i> (Grunow) Round and Basson (1997)
<i>Chaetoceros</i> (subgen. <i>Chaetoceros</i>) spp.	<i>Pennate</i> spp.
<i>Chaetoceros atlanticum</i> Cleve (1873)	<i>Pinnularia quadratarea</i> (A.Schmidt) Cleve (1895) *
<i>Chaetoceros</i> (subgen. <i>Hyalochaete</i>) spp.	<i>Pinnularia quadratarea</i> var. <i>cuneata</i> Østrup (1905) *
<i>Chaetoceros</i> spp. Restling Spores	<i>Pinnularia quadratarea</i> var. <i>dubia</i> Heiden (1905) *
<i>Coscinodiscus oculus-iridis</i> Ehrenberg (1839)	<i>Pinnularia semiinflata</i> (Østrup) Poulin and Cardinal (1982)
<i>Coscinodiscus radiatus</i> Enrenberg (1840)	<i>Pinnularia</i> spp.
<i>Craspedopleura kryophila</i> (Cleve) Poulin (1993) *	<i>Pleurosigma stuxbergii</i> Cleve and Grunow (1880) *
<i>Cyclotella</i> spp.	<i>Pleurosigma</i> spp.
<i>Cylindrotheca closterium</i> (Ehrenberg) Lewin and Reimann (1964)	<i>Pseudo-nitzschia</i> spp.
<i>Cymbella silesiaca</i> Bleisch (1864) ?	<i>Porosira glacialis</i> (Grunow) Jørgensen (1905) *
<i>Cymbella sinuata</i> Gregory (1858)	<i>Proboscia eumorpha</i> Takahashi, Jordan and Priddle (1994)
<i>Cymbella</i> spp.	<i>Pseudogomphonema arcticum</i> (Grunow) Medlin (1986)
<i>Delphineis</i> sp. cf. <i>angustata</i> (Pantocsek) Andrews (1981)	<i>Pseudogomphonema septentrionale</i> var. <i>angustatum</i> (Østrup) Medlin (1986) *
<i>Delphineis surirella</i> (Ehrenberg) Andrews (1981)	<i>Pseudogomphonema</i> spp.
<i>Diploneis littoralis</i> var. <i>clathrata</i> (Østrup) Cleve (1896) *	<i>Rhizosolenia borealis</i> Sundström (1986)
<i>Diploneis</i> sp. cf. <i>bombus</i> (Ehrenberg) Ehrenberg (1853)	<i>Rhizosolenia hebetata</i> Bailey (1856)
<i>Diploneis</i> spp.	<i>Rhizosolenia hebetata</i> f. <i>semispina</i> (Hensen) Gran (1904) ?
<i>Entomoneis</i> spp.	<i>Rhizosolenia setigera</i> Brightwell (1858)
<i>Eucampia groenlandica</i> Cleve (1896)	<i>Rhizosolenia</i> spp.
<i>Fossula arctica</i> Hasle, Syvertsen and Quillfeldt (1996) *	<i>Synedropsis hyperborea</i> (Grunow) Hasle, Medlin and Sybertsen (1994) *
<i>Fragilariopsis cylindrus</i> (Grunow) Krieger (1954) *	<i>Synedra</i> spp.
<i>Fragilariopsis oceanica</i> (Cleve) Hasle (1965) *	<i>Thalassiosira antarctica</i> Comber (1896) *
<i>Fragilariopsis</i> spp.	<i>Thalassiosira bioculata</i> (Grunow) Ostfeld (1903)
<i>Gyrosigma hudsonii</i> Poulin and Cardinal	<i>Thalassiosira decipiens</i> (Grunow) Jørgensen (1905) ?
<i>Gyrosigma macrum</i> (W.Smith) Cleve (1894) ?	<i>Thalassiosira eccentrica</i> (Ehrenberg) Cleve (1904) ?
<i>Haslea crucigeroides</i> (Hustedt) Simonsen (1974) *	<i>Thalassiosira hyalina</i> (Grunow) Gran (1897)
<i>Licmophora</i> sp.	<i>Thalassiosira hyperborea</i> (Grunow) Hasle (1989)
<i>Melosira arctica</i> Dickie (1852) *	<i>Thalassiosira leptopus</i> (Grunow) Hasle and Fryxell (1977)
<i>Melosira moniliformis</i> (Müller) Agardh (1824) ?	<i>Thalassiosira nordenskiöldii</i> Cleve (1873)
<i>Navicula algida</i> Grunow (1884) *	<i>Thalassiosira trifluta</i> Group
<i>Navicula directa</i> (Smith) Ralfs (1861)	<i>Thalassiosira</i> spp.
<i>Navicula distans</i> (Smith) Ralfs (1861)	<i>Thalassionema nitzschioides</i> (Grunow) Mereschkowsky (1902)
<i>Navicula forcipata</i> var. <i>densistriata</i> Schmidt (1881) ? *	<i>Thalassionema</i> spp. ?
<i>Navicula kariana</i> var. <i>detersa</i> Grunow (1882) *	<i>Thalassiothrix</i> sp.
<i>Navicula kryokonites</i> Cleve (1883) *	<i>Trachyneis aspera</i> (Ehrenberg) Cleve (1894)
<i>Navicula obtusa</i> Cleve (1883) *	
<i>Navicula superba</i> Cleve (1883) *	
<i>Navicula transitans</i> Cleve (1883) *	
<i>Navicula transitans</i> var. <i>detersa</i> (Grunow) Cleve (1883) *	
<i>Navicula valida</i> Cleve and Grunow (1880) *	
<i>Navicula</i> spp.	

Diatom flux reflects water-mass conditions

J. Onodera et al.

Title Page

Abstract

Introduction

Conclusions

References

Tables

Figures



Back

Close

Full Screen / Esc

Printer-friendly Version

Interactive Discussion



Table A1a. Sampling schedules for sediment trap deployments NAP10t and NAP11t, the bulk components, and diatom assemblage data of sediment trap samples from 4 October 2010 to 18 September 2012. The data periods are expanded from Watanabe et al. (2014). The event time on the dates of initial sampling and sample-cup closing is 0:00 LT (midnight). The symbol “–” indicates that the analysis was not conducted because of a limited sample volume. Methods for bulk component analyses are from Watanabe et al. (2014).

Sample ID	Initial Date (event time 0:00)	Close Date (event time 0:00)	Sampled Period (day)	Mean Depth of Moor- ed Sed. Trap (m)	Total Mass Flux (dry mg m ⁻² d ⁻¹)	Concentration (wt%)						Count Number of Diatom Valves (incl. Spores)
						Total Particulate Nitrogen	Particulate Organic Carbon	Organic Matter	CaCO ₃	Biogenic Opal	Lithogenic	
Shallow Trap												
NAP10t-S01	4 Oct 2010	18 Oct 2010	14	191.6 ± 2.4	0.1	–	–	–	–	–	–	–
NAP10t-S02	18 Oct 2010	2 Nov 2010	15	187.9 ± 2.0	43.0	0.9	6.4	18.4	4.7	15.2	61.7	712.5
NAP10t-S03	2 Nov 2010	17 Nov 2010	15	189.8 ± 7.2	150.8	0.6	5.2	14.8	2.2	17.9	65.1	1124.0
NAP10t-S04	17 Nov 2010	2 Dec 2010	15	190.3 ± 9.4	215.9	0.6	5.2	14.7	0.0	19.4	65.8	643.5
NAP10t-S05	2 Dec 2010	17 Dec 2010	15	189.9 ± 9.3	122.4	0.7	5.5	15.7	1.0	17.9	65.4	559.0
NAP10t-S06	17 Dec 2010	1 Jan 2011	15	187.1 ± 3.7	98.0	0.6	5.1	14.6	3.3	15.4	66.7	464.5
NAP10t-S07	1 Jan 2011	16 Jan 2011	15	186.5 ± 3.4	30.8	0.5	4.1	11.8	63.8	10.7	13.7	612.5
NAP10t-S08	16 Jan 2011	31 Jan 2011	15	184.9 ± 1.6	19.3	0.4	3.2	9.2	1.8	9.3	79.7	481.0
NAP10t-S09	31 Jan 2011	15 Feb 2011	15	184.5 ± 0.1	21.9	0.3	2.5	7.1	8.2	8.8	75.9	451.0
NAP10t-S10	15 Feb 2011	2 Mar 2011	15	184.5 ± 0.1	33.7	0.5	3.8	10.8	3.0	8.2	78.0	501.5
NAP10t-S11	2 Mar 2011	15 Mar 2011	13	184.5 ± 0.1	43.7	0.5	3.7	10.6	2.6	7.7	79.1	429.5
NAP10t-S12	15 Mar 2011	28 Mar 2011	13	184.5 ± 0.1	37.8	0.5	4.0	11.3	0.0	6.5	82.2	421.0
NAP10t-S13	28 Mar 2011	10 Apr 2011	13	185.5 ± 1.3	20.5	0.4	3.2	9.2	2.0	6.9	82.0	404.5
NAP10t-S14	10 Apr 2011	23 Apr 2011	13	186.0 ± 0.5	49.7	0.8	5.4	15.5	9.8	7.8	66.9	480.0
NAP10t-S15	23 Apr 2011	6 May 2011	13	184.7 ± 0.5	73.2	0.3	2.7	7.8	4.9	10.6	76.6	416.0
NAP10t-S16	6 May 2011	19 May 2011	13	184.4 ± 0.4	109.2	0.3	2.9	8.2	6.4	11.7	73.7	574.0
NAP10t-S17	19 May 2011	1 Jun 2011	13	184.3 ± 0.6	50.2	0.4	3.3	9.5	3.4	11.5	75.6	417.5
NAP10t-S18	1 Jun 2011	14 Jun 2011	13	184.4 ± 0.5	85.5	0.3	2.9	8.2	5.8	12.3	73.7	400.5
NAP10t-S19	14 Jun 2011	27 Jun 2011	13	184.0 ± 0.7	45.3	0.3	2.5	7.3	7.9	11.9	73.0	447.0
NAP10t-S20	27 Jun 2011	10 Jul 2011	13	184.0 ± 0.7	51.6	0.7	5.9	16.8	6.4	12.3	64.5	464.0
NAP10t-S21	10 Jul 2011	23 Jul 2011	13	184.1 ± 1.0	36.9	0.5	4.3	12.3	40.9	12.6	34.3	442.5
NAP10t-S22	23 Jul 2011	5 Aug 2011	13	184.0 ± 0.7	40.6	0.5	4.3	12.2	6.6	12.3	69.0	481.5
NAP10t-S23	5 Aug 2011	18 Aug 2011	13	184.4 ± 0.3	75.6	0.7	5.4	15.5	0.0	11.0	73.6	868.5
NAP10t-S24	18 Aug 2011	31 Aug 2011	13	186.0 ± 1.2	95.5	0.8	6.0	17.1	0.0	13.3	69.7	725.5
NAP10t-S25	31 Aug 2011	14 Sep 2011	14	190.9 ± 8.7	46.4	0.8	5.6	15.9	4.4	12.1	67.6	682.5
NAP10t-S26	14 Sep 2011	28 Sep 2011	14	187.4 ± 4.9	34.8	0.9	6.6	18.9	0.0	11.8	69.2	410.5

Table A1a. Continued.

Sample ID	Initial Date (event time 0:00)	Close Date (event time 0:00)	Sampled Period (day)	Mean Depth of Moor- ed Sed. Trap (m)	Total Mass Flux (dry mg m ⁻² d ⁻¹)	Concentration (wt%)						Count Number of Diatom Valves (incl. Spores)
						Total Particulate Nitrogen	Particulate Organic Carbon	Organic Matter	CaCO ₃	Biogenic Opal	Lithogenic	
Shallow Trap												
NAP11t-S01	4 Oct 2011	19 Oct 2011	15	258.1 ± 3.9	8.9	-	-	-	-	-	-	482.5
NAP11t-S02	19 Oct 2011	3 Nov 2011	15	259.1 ± 1.1	9.6	-	-	-	-	-	-	437.5
NAP11t-S03	3 Nov 2011	18 Nov 2011	15	258.3 ± 0.8	75.2	0.8	6.1	17.5	1.6	12.9	68.0	562.0
NAP11t-S04	18 Nov 2011	3 Dec 2011	15	259.2 ± 2.2	263.3	0.5	4.2	11.9	1.9	10.3	75.9	799.0
NAP11t-S05	3 Dec 2011	18 Dec 2011	15	256.9 ± 0.8	103.0	0.7	5.5	15.8	1.0	10.7	72.5	498.0
NAP11t-S06	18 Dec 2011	2 Jan 2012	15	257.8 ± 2.9	78.2	0.7	5.4	15.4	1.2	9.9	73.4	513.5
NAP11t-S07	2 Jan 2012	17 Jan 2012	15	256.5 ± 0.7	26.4	0.9	7.4	21.1	0.0	10.3	68.6	613.5
NAP11t-S08	17 Jan 2012	1 Feb 2012	15	256.8 ± 0.8	22.5	0.9	6.8	19.3	0.0	12.0	68.6	620.0
NAP11t-S09	1 Feb 2012	16 Feb 2012	15	256.2 ± 0.8	31.8	1.0	6.9	19.7	4.9	12.1	63.3	668.0
NAP11t-S10	16 Feb 2012	2 Mar 2012	15	257.6 ± 3.2	36.6	0.8	6.1	17.4	0.0	15.3	67.2	487.0
NAP11t-S11	2 Mar 2012	17 Mar 2012	15	257.6 ± 4.0	33.5	0.8	5.7	16.2	-	18.7	-	413.0
NAP11t-S12	17 Mar 2012	1 Apr 2012	15	254.8 ± 0.6	17.9	-	-	-	-	-	-	469.5
NAP11t-S13	1 Apr 2012	16 Apr 2012	15	254.6 ± 0.2	15.6	-	-	-	-	-	-	518.5
NAP11t-S14	16 Apr 2012	1 May 2012	15	254.5 ± 0.2	15.5	-	-	-	-	-	-	425.0
NAP11t-S15	1 May 2012	16 May 2012	15	256.5 ± 1.8	22.3	-	-	-	-	-	-	472.5
NAP11t-S16	16 May 2012	31 May 2012	15	257.0 ± 3.0	30.9	1.0	6.2	17.8	1.8	-	-	504.5
NAP11t-S17	31 May 2012	15 Jun 2012	15	255.9 ± 3.4	10.6	-	-	-	-	-	-	438.5
NAP11t-S18	15 Jun 2012	30 Jun 2012	15	254.2 ± 0.9	13.6	-	-	-	-	-	-	400.0
NAP11t-S19	30 Jun 2012	15 Jul 2012	15	260.5 ± 8.2	9.2	-	-	-	-	-	-	435.0
NAP11t-S20	10 Jul 2012	20 Jul 2012	10	300.0 ± 13.6	9.7	-	-	-	-	-	-	444.0
NAP11t-S21	20 Jul 2012	30 Jul 2012	10	307.0 ± 7.9	8.6	-	-	-	-	-	-	429.0
NAP11t-S22	30 Jul 2012	9 Aug 2012	10	277.9 ± 24.2	6.0	-	-	-	-	-	-	461.5
NAP11t-S23	9 Aug 2012	19 Aug 2012	10	253.8 ± 1.0	5.0	-	-	-	-	-	-	398.5
NAP11t-S24	19 Aug 2012	29 Aug 2012	10	253.3 ± 0.7	7.4	-	-	-	-	-	-	473.0
NAP11t-S25	29 Aug 2012	8 Sep 2012	10	253.0 ± 0.4	12.0	-	-	-	-	-	-	464.0
NAP11t-S26	8 Sep 2012	18 Sep 2012	10	252.9 ± 0.2	8.9	-	-	-	-	-	-	573.5

**Diatom flux reflects
water-mass
conditions**

J. Onodera et al.

Title Page

Abstract

Introduction

Conclusions

References

Tables

Figures

◀

▶

◀

▶

Back

Close

Full Screen / Esc

Printer-friendly Version

Interactive Discussion



Table A1a. Continued.

Sample ID	Initial Date (event time 0:00)	Close Date (event time 0:00)	Sampled Period (day)	Mean Depth of Moor- ed Sed. Trap (m)	Total Mass Flux (dry mg m ⁻² d ⁻¹)	Concentration (wt%)						Count Number of Diatom Valves (incl. Spores)
						Total Particulate Nitrogen	Particulate Organic Carbon	Organic Matter	CaCO ₃	Biogenic Opal	Lithogenic	
Deep Trap												
NAP10t-D01	4 Oct 2010	18 Oct 2010	14	1333.5 ± 2.3	2.4	-	-	-	-	-	-	80.0
NAP10t-D02	18 Oct 2010	2 Nov 2010	15	1329.1 ± 1.3	13.1	0.4	3.4	9.8	-	-	-	152.0
NAP10t-D03	2 Nov 2010	17 Nov 2010	15	1328.4 ± 2.6	53.1	0.5	4.1	11.7	-	14.0	-	417.0
NAP10t-D04	17 Nov 2010	2 Dec 2010	15	1327.5 ± 2.9	77.7	0.5	3.9	11.1	-	14.1	-	521.5
NAP10t-D05	2 Dec 2010	17 Dec 2010	15	1326.3 ± 3.0	116.9	0.4	3.4	9.6	7.0	15.3	68.1	440.0
NAP10t-D06	17 Dec 2010	1 Jan 2011	15	1324.8 ± 1.4	82.7	0.4	3.7	10.6	0.3	14.9	74.2	326.0
NAP10t-D07	1 Jan 2011	16 Jan 2011	15	1324.2 ± 1.3	39.6	0.3	2.8	8.0	0.7	13.5	77.9	341.5
NAP10t-D08	16 Jan 2011	31 Jan 2011	15	1323.0 ± 0.7	32.6	0.3	2.4	6.9	0.9	11.0	81.3	376.0
NAP10t-D09	31 Jan 2011	15 Feb 2011	15	1322.8 ± 0.4	37.9	0.3	2.9	8.3	1.7	9.9	80.0	416.0
NAP10t-D10	15 Feb 2011	2 Mar 2011	15	1322.7 ± 0.5	24.9	0.3	2.9	8.2	-	9.7	-	348.5
NAP10t-D11	2 Mar 2011	15 Mar 2011	13	1322.2 ± 0.8	23.7	0.2	2.1	5.9	-	8.7	-	330.0
NAP10t-D12	15 Mar 2011	28 Mar 2011	13	1322.2 ± 0.8	86.2	0.3	2.9	8.4	1.2	10.2	80.2	433.0
NAP10t-D13	28 Mar 2011	10 Apr 2011	13	1322.3 ± 1.2	50.6	0.3	2.7	7.6	1.3	9.2	82.0	331.5
NAP10t-D14	10 Apr 2011	23 Apr 2011	13	1322.6 ± 0.7	72.3	0.7	4.1	11.8	2.6	9.4	76.3	367.0
NAP10t-D15	23 Apr 2011	6 May 2011	13	1321.4 ± 0.5	41.3	0.5	3.4	9.7	1.4	8.8	80.1	322.5
NAP10t-D16	6 May 2011	19 May 2011	13	1321.1 ± 0.5	27.0	0.2	2.0	5.6	-	10.0	-	358.5
NAP10t-D17	19 May 2011	1 Jun 2011	13	1321.2 ± 0.4	62.3	0.3	2.4	6.8	1.9	9.7	81.5	371.5
NAP10t-D18	1 Jun 2011	14 Jun 2011	13	1321.1 ± 0.5	27.4	0.3	2.4	6.7	-	10.0	-	370.0
NAP10t-D19	14 Jun 2011	27 Jun 2011	13	1320.8 ± 0.7	17.7	0.2	1.7	5.0	2.3	9.2	83.6	181.5
NAP10t-D20	27 Jun 2011	10 Jul 2011	13	1320.3 ± 0.8	19.1	0.2	1.9	5.3	2.0	8.0	84.7	140.5
NAP10t-D21	10 Jul 2011	23 Jul 2011	13	1320.0 ± 0.7	44.3	0.2	2.1	6.1	1.2	7.9	84.8	365.5
NAP10t-D22	23 Jul 2011	5 Aug 2011	13	1319.6 ± 0.3	106.8	0.3	3.1	8.9	1.4	8.4	81.3	369.0
NAP10t-D23	5 Aug 2011	18 Aug 2011	13	1319.5 ± 0.5	160.2	0.4	3.6	10.3	2.7	9.1	77.9	475.5
NAP10t-D24	18 Aug 2011	31 Aug 2011	13	1319.8 ± 0.6	110.3	0.4	3.7	10.5	3.0	10.9	75.6	417.0
NAP10t-D25	31 Aug 2011	14 Sep 2011	14	1321.5 ± 2.9	75.5	0.5	4.0	11.4	1.9	10.9	75.8	452.5
NAP10t-D26	14 Sep 2011	28 Sep 2011	14	1320.1 ± 1.8	53.7	0.4	3.2	9.0	0.5	10.7	-	-

**Diatom flux reflects
water-mass
conditions**

J. Onodera et al.

[Title Page](#)

[Abstract](#)

[Introduction](#)

[Conclusions](#)

[References](#)

[Tables](#)

[Figures](#)



[Back](#)

[Close](#)

[Full Screen / Esc](#)

[Printer-friendly Version](#)

[Interactive Discussion](#)



Table A1a. Continued.

Sample ID	Initial Date (event time 0:00)	Close Date (event time 0:00)	Sampled Period (day)	Mean Depth of Moor- ed Sed. Trap (m)	Total Mass Flux (dry mg m ⁻² d ⁻¹)	Concentration (wt%)						Count Number of Diatom Valves (incl. Spores)
						Total Particulate Nitrogen	Particulate Organic Carbon	Organic Matter	CaCO ₃	Biogenic Opal	Lithogenic	
NAP11t-D01	4 Oct 2011	19 Oct 2011	15	1363.5 ± 1.3	26.4	-	-	-	-	-	-	414.0
NAP11t-D02	19 Oct 2011	3 Nov 2011	15	1361.8 ± 0.6	24.4	-	-	-	-	-	-	395.5
NAP11t-D03	3 Nov 2011	18 Nov 2011	15	1361.1 ± 1.1	36.4	0.6	4.6	13.0	-	10.7	-	403.5
NAP11t-D04	18 Nov 2011	3 Dec 2011	15	1360.8 ± 1.2	115.6	0.4	3.6	10.2	0.5	11.3	78.0	507.5
NAP11t-D05	3 Dec 2011	18 Dec 2011	15	1359.7 ± 0.2	114.8	0.4	3.5	10.1	1.0	11.0	77.8	554.0
NAP11t-D06	18 Dec 2011	2 Jan 2012	15	1360.0 ± 0.9	100.3	0.4	3.8	10.9	1.0	11.3	76.7	472.5
NAP11t-D07	2 Jan 2012	17 Jan 2012	15	1359.7 ± 0.0	85.5	0.4	3.8	10.7	1.8	11.6	76.0	505.0
NAP11t-D08	17 Jan 2012	1 Feb 2012	15	1359.7 ± 0.0	54.1	0.4	3.8	11.0	1.0	11.1	77.0	446.0
NAP11t-D09	1 Feb 2012	16 Feb 2012	15	1359.7 ± 0.0	38.7	0.4	3.9	11.2	0.1	10.1	78.6	-
NAP11t-D10	16 Feb 2012	2 Mar 2012	15	1360.1 ± 0.8	15.3	-	-	-	-	-	-	-
NAP11t-D11	2 Mar 2012	17 Mar 2012	15	1360.1 ± 1.0	1.6	-	-	-	-	-	-	-
NAP11t-D12	17 Mar 2012	1 Apr 2012	15	1359.6 ± 0.5	8.0	-	-	-	-	-	-	355.0
NAP11t-D13	1 Apr 2012	16 Apr 2012	15	1359.5 ± 0.7	4.1	-	-	-	-	-	-	423.5
NAP11t-D14	16 Apr 2012	1 May 2012	15	1359.4 ± 0.8	6.3	-	-	-	-	-	-	431.5
NAP11t-D15	1 May 2012	16 May 2012	15	1359.7 ± 0.4	1.0	-	-	-	-	-	-	-
NAP11t-D16	16 May 2012	31 May 2012	15	1359.9 ± 0.9	1.1	-	-	-	-	-	-	-
NAP11t-D17	31 May 2012	15 Jun 2012	15	1359.7 ± 1.2	0.0	-	-	-	-	-	-	-
NAP11t-D18	15 Jun 2012	30 Jun 2012	15	1359.1 ± 1.0	< 0.01	-	-	-	-	-	-	-
NAP11t-D19	30 Jun 2012	15 Jul 2012	15	1360.9 ± 2.5	< 0.01	-	-	-	-	-	-	-
NAP11t-D20	10 Jul 2012	20 Jul 2012	10	1372.9 ± 4.2	0.7	-	-	-	-	-	-	-
NAP11t-D21	20 Jul 2012	30 Jul 2012	10	1375.1 ± 2.6	< 0.01	-	-	-	-	-	-	-
NAP11t-D22	30 Jul 2012	9 Aug 2012	10	1366.4 ± 7.3	0.3	-	-	-	-	-	-	-
NAP11t-D23	9 Aug 2012	19 Aug 2012	10	1359.1 ± 1.0	< 0.01	-	-	-	-	-	-	-
NAP11t-D24	19 Aug 2012	29 Aug 2012	10	1359.2 ± 1.0	2.5	-	-	-	-	-	-	-
NAP11t-D25	29 Aug 2012	8 Sep 2012	10	1358.8 ± 1.1	3.6	-	-	-	-	-	-	-
NAP11t-D26	8 Sep 2012	18 Sep 2012	10	1358.8 ± 1.1	0.9	-	-	-	-	-	-	-

Diatom flux reflects water-mass conditions

J. Onodera et al.

Title Page

Abstract

Introduction

Conclusions

References

Tables

Figures

◀

▶

◀

▶

Back

Close

Full Screen / Esc

Printer-friendly Version

Interactive Discussion



Table A1b. Sampling schedules for sediment trap deployments NAP10t and NAP11t, the bulk components, and diatom assemblage data of sediment trap samples from 4 October 2010 to 18 September 2012. The data periods are expanded from Watanabe et al. (2014). The event time on the dates of initial sampling and sample-cup closing is 0:00 LT (midnight). The symbol “–” indicates that the analysis was not conducted because of a limited sample volume. Methods for bulk component analyses are from Watanabe et al. (2014).

Sample ID	Diatom Valve Flux ($\times 10^5$ valves $m^{-2} d^{-1}$)			Relative Valve Abundance without Chatoceros Resting Spores in Total Diatoms (%)										
	Total Diatom Flux	Sea-ice Related Taxa	Other Diatoms	<i>Chaetoceros</i> Resting Spores	% <i>Chaetoceros</i> spp.	% <i>Rhizosolenia</i> spp. and <i>Proboscia</i> spp.	% <i>Thalassisira</i> spp.	%Other Centric	% <i>Fossula arctica</i>	% <i>Fragilariopsis</i> spp.	% <i>Nitzschia</i> spp.	% <i>Thalassionema nitzschioides</i>	% <i>Neodenticula seminata</i>	%Other Pennates
Shallow Trap														
NAP10t-S01	–	–	–	–	–	–	–	–	–	–	–	–	–	–
NAP10t-S02	26.5	1.6	10.2	14.7	13.6	3.2	5.7	4.7	3.8	4.1	1.6	52.9	0.0	10.4
NAP10t-S03	76.2	3.4	27.1	45.7	16.7	5.3	8.7	6.0	5.3	4.4	2.0	46.1	0.0	5.4
NAP10t-S04	175.4	3.8	60.1	111.5	53.3	0.4	3.0	5.5	3.8	1.7	0.0	29.2	0.0	3.
NAP10t-S05	84.7	2.4	29.2	53.0	27.3	1.0	5.7	7.7	2.9	3.3	2.9	42.1	0.0	7.2
NAP10t-S06	118.7	1.8	55.6	61.3	42.8	1.8	2.7	8.5	1.3	0.9	0.9	35.4	0.0	5.8
NAP10t-S07	27.7	0.4	13.3	14.0	29.4	1.0	3.6	10.6	0.0	1.3	1.3	49.4	0.0	3.3
NAP10t-S08	13.0	0.1	6.5	6.5	28.1	0.0	4.1	8.7	0.0	0.0	1.2	56.6	0.0	1.2
NAP10t-S09	12.2	0.3	6.3	5.6	16.0	0.0	8.2	6.6	3.3	0.0	1.2	60.7	0.0	4.1
NAP10t-S10	11.3	0.2	6.1	5.0	14.7	1.1	5.0	9.3	1.1	0.7	1.4	63.1	0.0	3.6
NAP10t-S11	13.4	0.4	8.3	4.8	11.9	1.1	6.5	9.0	2.2	0.7	1.1	65.6	0.0	1.8
NAP10t-S12	9.4	0.3	5.1	4.0	11.5	0.8	5.7	7.4	0.8	2.9	0.0	69.9	0.0	1.
NAP10t-S13	7.9	0.2	4.1	3.5	6.3	0.4	8.9	11.2	2.7	0.4	0.0	66.4	0.4	3.1
NAP10t-S14	15.0	1.4	6.8	6.8	5.7	0.4	9.2	15.3	5.3	6.9	2.3	47.1	0.0	7.8
NAP10t-S15	21.7	2.2	8.1	11.4	4.0	0.5	8.1	7.1	5.6	13.6	3.0	48.5	0.0	9.6
NAP10t-S16	22.4	2.2	6.1	14.1	1.4	1.9	5.6	6.5	7.5	18.2	3.7	45.6	0.0	9.6
NAP10t-S17	16.3	1.7	4.7	10.0	0.0	1.2	5.5	6.8	11.1	11.1	1.2	51.4	0.0	11.7
NAP10t-S18	20.9	2.8	7.6	10.4	3.5	0.0	7.0	9.0	6.0	17.5	5.5	38.7	0.0	13.
NAP10t-S19	14.0	2.2	4.8	7.0	2.7	1.8	10.8	7.2	9.4	18.8	6.3	34.1	0.0	9.
NAP10t-S20	14.5	1.8	5.1	7.6	0.0	1.8	11.8	13.1	7.2	13.1	3.6	32.6	0.0	16.7
NAP10t-S21	17.3	6.1	4.8	6.4	0.4	1.4	5.0	7.2	27.5	25.8	0.0	15.6	0.0	17.2
NAP10t-S22	15.1	3.4	4.5	7.2	2.8	1.2	1.6	9.5	19.9	13.1	17.5	9.7	0.0	24.7

Table A1b. Continued.

Sample ID	Diatom Valve Flux ($\times 10^5$ valves $m^{-2} d^{-1}$)				Relative Valve Abundance without Chatoceros Resting Spores in Total Diatoms (%)									
	Total Diatom Flux	Sea-ice Related Taxa	Other Diatoms	Chaetoceros Resting Spores	%Chaetoceros spp.	%Rhizosolenia spp. and Proboscia spp.	%Thalassisira spp.	%Other Centric	%Fossula arctica	%Fragilaritopsis spp.	%Nitzschia spp.	%Thalassionema nitzschoides	%Neodenticula seminiae	%Other Pennates
NAP10t-S23	67.9	42.6	10.3	15.0	1.3	0.0	2.1	2.2	66.7	11.7	3.1	2.1	0.0	10.8
NAP10t-S24	113.4	85.2	8.2	20.0	0.3	0.0	1.5	2.5	77.5	12.6	1.2	0.8	0.0	3.7
NAP10t-S25	49.6	30.2	8.1	11.3	0.2	1.3	1.9	4.4	73.0	5.9	1.1	2.2	0.0	10.
NAP10t-S26	29.8	18.8	3.8	7.2	1.6	0.3	0.6	5.8	79.9	2.6	1.0	4.0	0.0	4.2
NAP11t-S01	4.4	1.4	1.7	1.2	3.8	36.8	5.5	2.6	39.1	4.1	2.6	2.7	0.0	2.9
NAP11t-S02	1.7	0.4	0.6	0.6	10.3	28.6	3.3	6.6	31.2	5.9	2.9	6.8	0.0	4.4
NAP11t-S03	3.8	4.8	21.6	11.7	4.4	52.6	4.4	2.3	14.9	2.6	3.3	14.6	0.0	1.
NAP11t-S04	108.3	5.6	66.0	36.7	53.8	10.8	4.7	2.8	6.8	0.0	2.1	16.1	0.0	2.8
NAP11t-S05	67.5	4.9	37.3	25.3	42.8	2.6	2.6	5.1	5.8	2.9	4.5	31.8	0.0	1.9
NAP11t-S06	34.8	3.8	14.1	16.9	33.3	3.0	8.7	7.9	12.1	4.2	0.0	27.8	0.0	3.
NAP11t-S07	13.9	1.4	7.1	5.3	25.6	7.1	7.1	5.5	11.1	1.8	1.6	36.5	0.0	3.7
NAP11t-S08	14.0	1.0	6.8	6.1	24.7	1.7	6.3	6.9	3.7	4.3	3.7	43.4	0.3	4.9
NAP11t-S09	15.1	1.0	7.2	6.9	23.6	4.1	5.8	5.2	7.1	2.5	0.8	47.3	0.0	3.6
NAP11t-S10	11.0	0.9	4.3	5.9	17.5	1.3	8.8	6.6	8.3	5.7	0.9	46.5	0.0	4.4
NAP11t-S11	9.3	0.7	3.7	5.0	6.3	2.1	12.0	9.9	6.3	1.6	2.6	53.6	0.0	5.7
NAP11t-S12	5.3	0.5	2.2	2.7	11.6	2.6	10.8	8.6	12.9	2.6	2.6	44.9	0.0	3.4
NAP11t-S13	4.7	0.4	2.0	2.4	11.3	2.3	13.3	7.0	3.9	5.1	3.5	47.0	0.0	6.6
NAP11t-S14	4.8	0.5	2.0	2.3	5.4	3.6	4.5	6.8	8.1	5.0	3.6	37.1	0.5	25.3
NAP11t-S15	5.3	0.6	2.3	2.5	5.6	0.4	12.0	12.4	5.2	5.6	7.2	45.9	0.0	5.6
NAP11t-S16	8.5	0.6	1.9	6.1	4.9	4.9	7.0	12.5	12.5	6.3	6.3	40.8	0.0	4.9
NAP11t-S17	2.5	0.2	0.9	1.4	6.0	0.5	7.6	9.3	5.4	3.8	5.4	52.0	0.0	9.8
NAP11t-S18	2.6	0.2	1.2	1.2	4.2	2.8	7.5	12.1	8.9	3.7	1.9	53.5	0.0	5.4
NAP11t-S19	29.5	2.0	13.1	14.4	6.7	2.2	10.3	6.7	5.8	4.9	2.7	54.7	0.0	5.8
NAP11t-S20	18.1	4.1	8.9	5.1	0.9	2.8	10.1	6.3	1.6	8.5	20.4	25.8	0.0	23.6
NAP11t-S21	21.8	3.0	12.8	6.0	1.0	2.6	7.4	11.3	1.0	2.9	16.4	27.7	0.0	29.9
NAP11t-S22	15.6	1.9	9.3	4.4	3.3	1.8	15.7	22.1	2.1	1.5	12.7	21.0	0.0	19.7
NAP11t-S23	10.1	0.8	7.0	2.3	8.2	1.3	30.3	9.8	2.0	0.7	7.2	20.4	0.0	20.2
NAP11t-S24	24.0	2.5	17.6	3.9	3.8	1.0	35.1	11.1	0.3	0.8	8.8	22.7	0.0	16.4
NAP11t-S25	15.7	1.6	10.7	3.4	9.6	0.8	19.0	16.3	3.3	0.3	8.0	20.7	0.0	22.
NAP11t-S26	29.1	2.7	18.5	7.9	7.9	1.9	33.0	16.5	1.7	0.2	9.1	17.3	0.0	12.4

Diatom flux reflects water-mass conditions

J. Onodera et al.

Title Page

Abstract

Introduction

Conclusions

References

Tables

Figures

⏪

⏩

◀

▶

Back

Close

Full Screen / Esc

Printer-friendly Version

Interactive Discussion



Table A1b. Continued.

Sample ID	Diatom Valve Flux ($\times 10^5$ valves $m^{-2} d^{-1}$)			Relative Valve Abundance without Chatoceros Resting Spores in Total Diatoms (%)										
	Total Diatom Flux	Sea-ice Related Taxa	Other Diatoms	<i>Chaetoceros</i> Resting Spores	% <i>Chaetoceros</i> spp.	% <i>Rhizosolenia</i> spp. and <i>Proboscia</i> spp.	% <i>Thalassisira</i> spp.	%Other Centric	% <i>Fossula arctica</i>	% <i>Fragilariopsis</i> spp.	% <i>Nitzschia</i> spp.	% <i>Thalassionema nitzschioides</i>	% <i>Neodenticula seminiae</i>	%Other Pennates
Deep Trap														
NAP10t-D01	0.6	0.0	0.4	0.1	1.6	6.5	8.1	29.0	0.0	3.2	14.5	7.3	13.0	16.8
NAP10t-D02	1.0	0.2	0.5	0.3	10.2	4.6	15.7	12.0	6.5	7.4	10.2	22.2	0.0	11.1
NAP10t-D03	11.3	1.4	4.4	5.6	3.8	1.4	10.4	9.0	8.5	11.3	7.5	37.5	0.0	10.6
NAP10t-D04	11.8	1.7	5.1	5.0	10.4	1.7	2.3	10.4	11.0	10.4	3.0	40.2	0.0	10.7
NAP10t-D05	29.8	2.4	12.8	14.6	25.4	2.7	4.0	9.8	6.3	7.6	1.3	38.4	0.0	4.5
NAP10t-D06	22.1	2.1	10.0	10.0	17.3	1.1	7.3	5.6	5.0	8.9	1.1	42.5	0.0	11.2
NAP10t-D07	11.6	1.3	4.7	5.6	14.2	2.3	11.9	3.4	6.8	11.3	1.7	41.6	0.0	6.8
NAP10t-D08	12.7	0.8	6.0	5.9	38.1	0.5	9.4	5.0	5.4	3.5	2.5	30.9	0.0	4.7
NAP10t-D09	14.1	0.6	8.8	4.7	41.9	1.4	11.6	5.4	1.8	2.5	1.8	31.2	0.0	2.3
NAP10t-D10	9.4	0.7	5.2	3.5	29.7	0.0	6.9	5.0	5.9	3.2	1.8	43.5	0.0	3.9
NAP10t-D11	5.2	0.4	3.2	1.5	26.0	1.3	10.0	4.3	5.2	2.6	4.3	40.9	0.0	5.4
NAP10t-D12	16.9	1.4	10.7	4.8	29.8	1.6	7.4	5.8	4.9	2.9	1.6	42.4	0.0	3.6
NAP10t-D13	10.4	0.9	6.0	3.5	30.4	0.0	13.2	9.1	3.2	4.5	1.8	36.5	0.0	1.4
NAP10t-D14	14.3	1.7	7.9	4.8	19.6	0.8	10.2	3.7	11.8	2.0	1.2	40.0	0.4	10.2
NAP10t-D15	4.6	0.7	2.5	1.4	5.8	0.4	15.7	5.4	13.5	4.0	3.6	37.5	0.4	13.5
NAP10t-D16	5.6	1.0	2.4	2.3	9.8	2.3	6.6	7.0	10.8	11.7	6.1	33.5	0.0	12.2
NAP10t-D17	7.3	1.2	3.2	2.9	14.8	0.4	6.3	9.4	8.5	14.3	11.2	22.6	0.0	12.5
NAP10t-D18	7.2	1.1	3.3	2.9	14.9	1.4	8.1	11.3	9.5	13.5	4.5	30.2	0.0	6.8
NAP10t-D19	2.8	0.5	1.2	1.2	21.8	0.0	9.5	9.5	12.3	6.6	5.7	24.2	0.0	10.4
NAP10t-D20	2.2	0.1	1.1	1.0	7.8	1.3	1.3	9.2	6.5	2.6	1.3	62.1	0.0	7.8
NAP10t-D21	8.2	1.0	4.7	2.5	8.6	0.0	5.1	7.1	6.3	9.0	5.1	52.1	0.0	6.7
NAP10t-D22	11.5	2.0	5.8	3.7	7.6	0.8	6.0	6.4	9.2	13.5	5.2	40.6	0.0	10.8
NAP10t-D23	37.2	19.8	8.4	9.0	1.9	0.6	6.4	6.1	56.6	8.9	6.7	8.2	0.0	4.7
NAP10t-D24	65.2	49.9	5.9	9.4	0.6	0.0	1.7	2.5	75.9	12.9	0.6	2.5	0.0	3.4
NAP10t-D25	32.9	20.6	6.9	5.3	1.8	0.3	7.4	2.9	62.5	11.1	3.4	5.1	0.0	5.5

Table A1b. Continued.

Sample ID	Diatom Valve Flux ($\times 10^5$ valves $m^{-2} d^{-1}$)			Relative Valve Abundance without Chatoceros Resting Spores in Total Diatoms (%)										
	Total Diatom Flux	Sea-ice Related taxa	Other Diatoms	<i>Chaetoceros</i> Resting Spores	% <i>Chaetoceros</i> spp.	% <i>Rhizosolenia</i> spp. and <i>Proboscia</i> spp.	% <i>Thalassisira</i> spp.	%Other Centric	% <i>Fossula arctica</i>	% <i>Fragilariopsis</i> spp.	% <i>Nitzschia</i> spp.	% <i>Thalassionema nitzschioides</i>	% <i>Neodenticula seminiae</i>	%Other Pennates
NAP10t-D26	-	-	-	-	-	-	-	-	-	-	-	-	-	-
NAP11t-D01	4.6	2.6	1.2	0.8	2.9	0.9	2.0	8.8	53.4	12.0	2.9	9.8	0.6	6.7
NAP11t-D02	6.7	4.0	1.3	1.4	1.0	2.9	4.5	5.8	64.8	8.7	4.8	6.1	0.0	1.3
NAP11t-D03	7.8	3.6	2.3	1.9	3.0	2.0	4.0	10.9	50.4	9.2	5.3	11.2	0.0	4.1
NAP11t-D04	22.8	6.0	7.4	9.5	21.7	5.1	2.4	6.1	36.9	7.1	0.7	14.4	0.0	5.8
NAP11t-D05	37.4	6.0	15.2	16.2	38.3	4.8	10.9	6.4	24.3	2.9	0.6	11.2	0.0	0.6
NAP11t-D06	31.9	3.7	14.2	14.0	39.3	3.8	4.9	7.2	15.5	4.2	1.1	21.7	0.0	2.3
NAP11t-D07	9.7	2.3	3.9	3.5	18.4	2.8	5.3	10.0	29.0	5.9	1.6	21.8	0.0	5.3
NAP11t-D08	15.0	1.9	8.7	4.4	43.8	4.2	1.3	6.4	13.1	3.8	1.6	21.4	0.0	4.5
NAP11t-D09	-	-	-	-	-	-	-	-	-	-	-	-	-	-
NAP11t-D10	-	-	-	-	-	-	-	-	-	-	-	-	-	-
NAP11t-D11	-	-	-	-	-	-	-	-	-	-	-	-	-	-
NAP11t-D12	3.7	0.6	2.1	1.1	31.6	6.4	3.6	7.2	15.2	4.8	0.4	27.0	0.0	3.8
NAP11t-D13	2.0	0.4	1.1	0.6	32.6	6.9	6.2	5.9	19.9	6.2	0.3	18.1	0.7	3.3
NAP11t-D14	2.1	0.4	1.0	0.7	31.4	5.5	8.3	5.9	16.9	8.6	0.7	16.2	0.7	5.7
NAP11t-D15	-	-	-	-	-	-	-	-	-	-	-	-	-	-
NAP11t-D16	-	-	-	-	-	-	-	-	-	-	-	-	-	-
NAP11t-D17	-	-	-	-	-	-	-	-	-	-	-	-	-	-
NAP11t-D18	-	-	-	-	-	-	-	-	-	-	-	-	-	-
NAP11t-D19	-	-	-	-	-	-	-	-	-	-	-	-	-	-
NAP11t-D20	-	-	-	-	-	-	-	-	-	-	-	-	-	-
NAP11t-D21	-	-	-	-	-	-	-	-	-	-	-	-	-	-
NAP11t-D22	-	-	-	-	-	-	-	-	-	-	-	-	-	-
NAP11t-D23	-	-	-	-	-	-	-	-	-	-	-	-	-	-
NAP11t-D24	-	-	-	-	-	-	-	-	-	-	-	-	-	-
NAP11t-D25	-	-	-	-	-	-	-	-	-	-	-	-	-	-
NAP11t-D26	-	-	-	-	-	-	-	-	-	-	-	-	-	-

Diatom flux reflects water-mass conditions

J. Onodera et al.

Title Page

Abstract Introduction

Conclusions References

Tables Figures

◀ ▶

◀ ▶

Back Close

Full Screen / Esc

Printer-friendly Version

Interactive Discussion



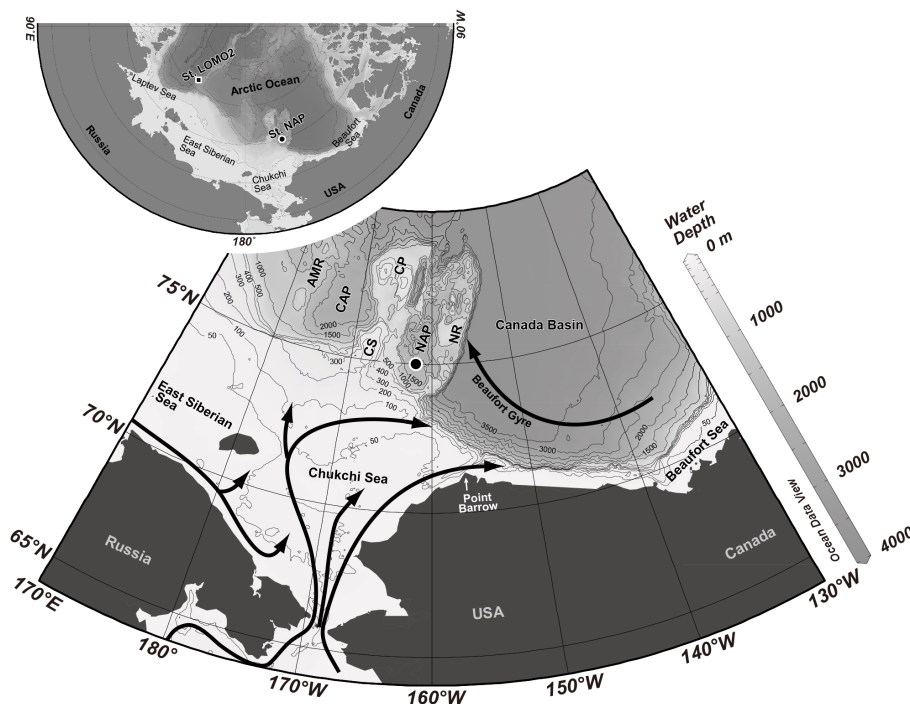


Figure 1. Bathymetric map around Station NAP (solid black circle at 75° N, 162° W) in the western Arctic Ocean, and schematic of sea-surface circulation over the Chukchi Sea shelf and in the southern Canada Basin (Danielson et al., 2011). NR, Northwind Ridge; NAP, Northwind Abyssal Plain; CP, Chukchi Plateau; CS, Chukchi Spur; CAP, Chukchi Abyssal Plain; AMR, Alpha-Mendeleev Ridge complex.

Diatom flux reflects water-mass conditions

J. Onodera et al.

Title Page

Abstract

Introduction

Conclusions

References

Tables

Figures

◀

▶

◀

▶

Back

Close

Full Screen / Esc

Printer-friendly Version

Interactive Discussion



Diatom flux reflects water-mass conditions

J. Onodera et al.

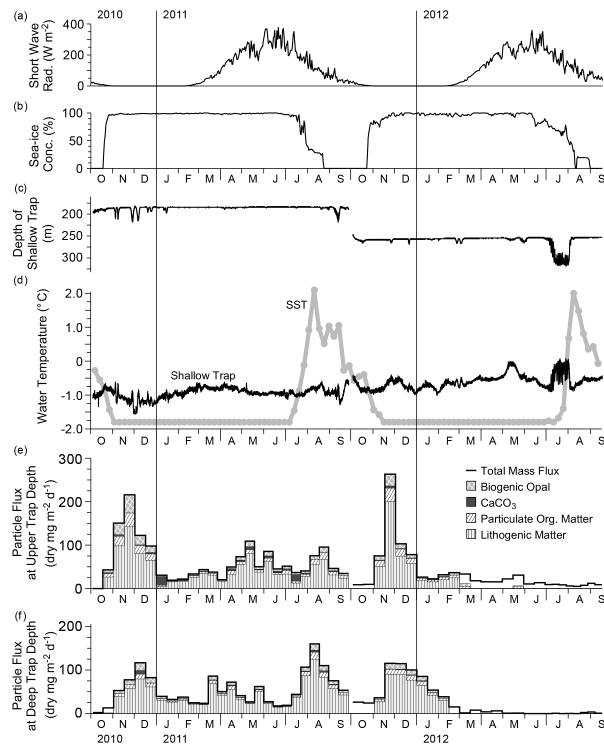


Figure 2. Time-series data at Station NAP from 1 October 2010 through 18 September 2012. **(a)** Climate Forecast System Reanalysis (CFSR) reanalysis data of shortwave radiation, **(b)** CFSR reanalysis data of sea-ice concentration, **(c)** depth log of moored shallow trap, **(d)** water temperature recorded at moored shallow trap (black line), and NOAA OI.v2 weekly sea-surface temperature at Station NAP (gray line), **(e)** total mass flux and bulk components of sinking particles at shallow trap depth (data period was expanded from Watanabe et al., 2014), and **(f)** total mass flux and bulk components at deep trap depth. Blank areas in bulk component data indicate no analysis because of limited sample volume.

Title Page

Abstract

Introduction

Conclusions

References

Tables

Figures



Back

Close

Full Screen / Esc

Printer-friendly Version

Interactive Discussion



Diatom flux reflects
water-mass
conditions

J. Onodera et al.

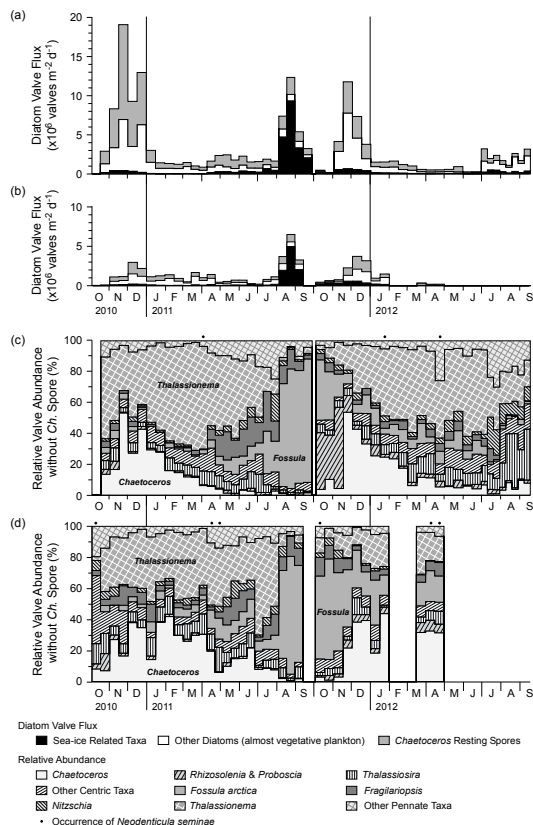


Figure 3. Total diatom flux and settling diatom assemblage at Station NAP from 4 October 2010 through 17 September 2012. **(a)** Sinking diatom flux at shallow trap, **(b)** sinking diatom flux at deep trap, **(c)** relative diatom valve abundance excluding *Chaetoceros* spores at shallow trap, and **(d)** relative diatom valve abundance excluding *Chaetoceros* spores at deep trap. Blanks in time-series data indicate periods with no data because of limited sample volume or periods without sampling because of mooring turnaround. The plot data is listed in Table A1.

Title Page

Abstract

Introduction

Conclusions

References

Tables

Figures



Back

Close

Full Screen / Esc

Printer-friendly Version

Interactive Discussion



Diatom flux reflects water-mass conditions

J. Onodera et al.

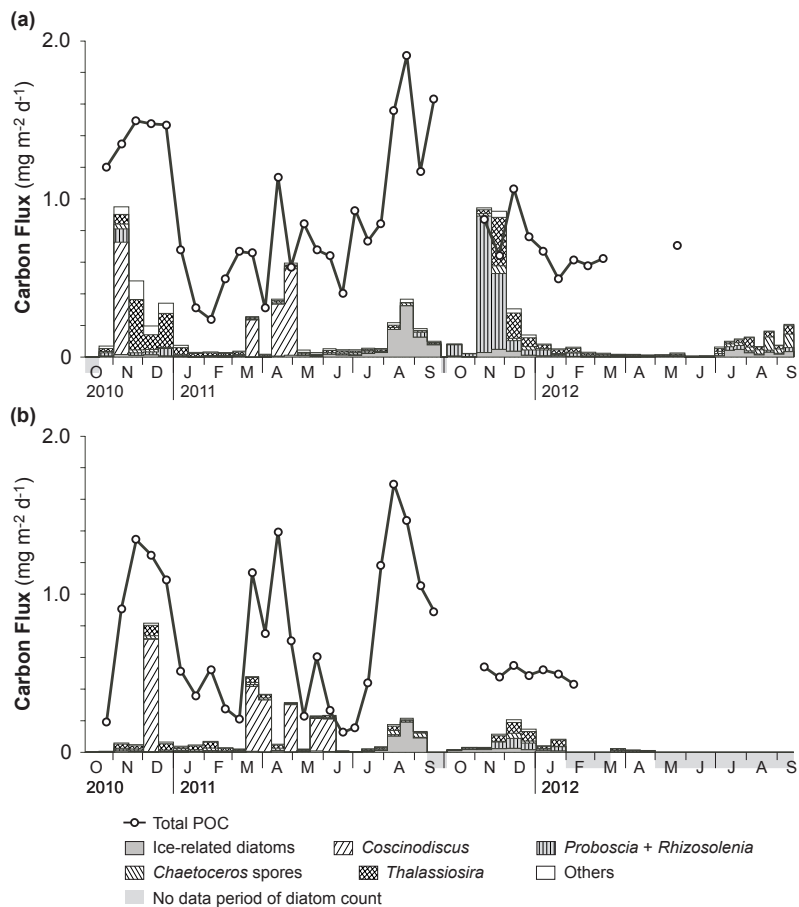


Figure 4. Time-series fluxes of total POC and diatom-derived carbon at Station NAP. **(a)** Shallow trap, and **(b)** deep trap.

Diatom flux reflects water-mass conditions

J. Onodera et al.

Title Page

Abstract

Introduction

Conclusions

References

Tables

Figures



Back

Close

Full Screen / Esc

Printer-friendly Version

Interactive Discussion

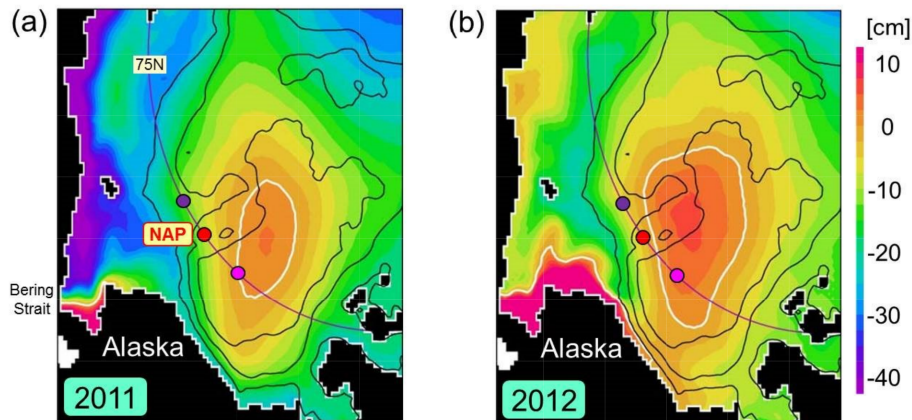


Figure 5. Sea surface height (cm) in the western Arctic Ocean obtained from the COCO model. The summertime averages over June, July, and August are shown for (a) 2011 and (b) 2012. Black contours trace isobaths of 100, 1000, and 3000 m. The white contours indicate a sea surface height of zero. The purple line corresponds to 75° N, used for modeled current direction in Fig. 6. Red dots show the location of Station NAP. Purple dots represent the east and west limits of the horizontal section in Fig. 6.

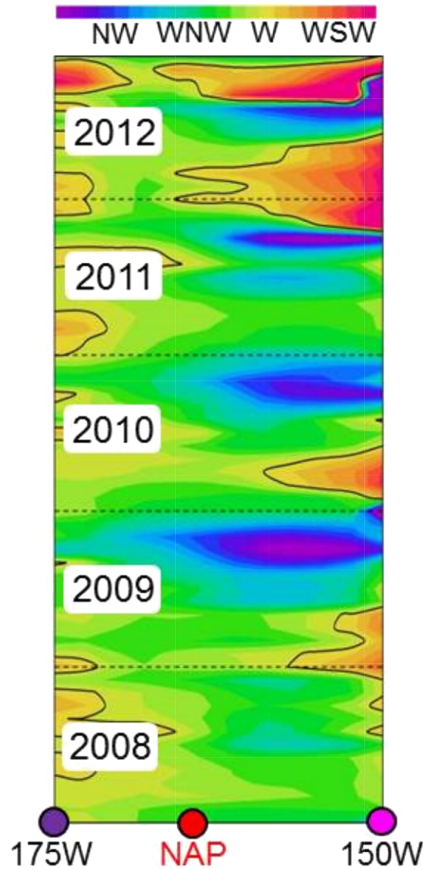


Figure 6. Modeled ocean current direction averaged from the surface to 100 m depth across an east–west section along 75° N (see purple line in Fig. 5). The vertical axis represents an inter-annual time-series from 2008 to 2012. Blue (red) color indicates a northwestward (southwestward) ocean current.

BGD

11, 15215–15250, 2014

Diatom flux reflects water-mass conditions

J. Onodera et al.

Title Page

Abstract

Introduction

Conclusions

References

Tables

Figures



Back

Close

Full Screen / Esc

Printer-friendly Version

Interactive Discussion

